

1 **A three year time-series of volatile organic iodocarbons in Bedford Basin, Nova Scotia :**
2 **a Northwestern Atlantic fjord.**

3
4 *Qiang Shi¹, Douglas Wallace¹*

5
6 ¹Department of Oceanography, Dalhousie University, Halifax, Canada
7 Email: qshi@dal.ca

8
9 **Abstract:**

10
11 We report weekly observations of volatile organic iodocarbons (CH₃I, CH₂ClI and CH₂I₂) over the
12 time-period May 2015 to December 2017 from 4 depths in Bedford Basin, a coastal fjord (70m
13 deep) on the Atlantic coast of Canada. The fjord is subject to winter-time mixing, seasonal
14 stratification and bloom dynamics, subsurface oxygen depletion, local input of freshwater and
15 occasional intrusions of higher density water from the adjacent continental shelf. Near-surface
16 concentrations showed strong seasonal and sub-seasonal variability which is compared with other
17 coastal time-series. The vertical variation of CH₂I₂ and CH₂ClI within the upper 10m is consistent
18 with rapid photolysis of CH₂I₂. Average annual sea-to-air fluxes (46.7 nmol m⁻² day⁻¹) of total
19 volatile organic iodine were similar to those observed in other coastal and shelf time-series and
20 polyiodinated compounds contributed 80% of the total flux. Fluxes were subject to strong
21 interannual variability (a factor of two) mainly due to wind-speed variability. Near-surface net
22 production of CH₃I averaged 1 pmol L⁻¹ day⁻¹ and was similar to rates in the English Channel but
23 an order of magnitude higher than in shallow waters of the Kiel Fjord, Germany, possibly due to
24 higher microbial degradation in the latter. The near-bottom (60 m) time-series showed evidence
25 for CH₃I production associated with organic matter degradation, and a possible “switch” from
26 production of CH₃I via an alkylation pathway to production of CH₂I₂ by a haloform-type reaction.
27 Near-bottom CH₃I production varied strongly between years but was generally ca. 20 times lower
28 than near-surface production.

1 **Keywords:** Iodocarbons, iodomethane, chloriodomethane, diiodomethane, air-sea flux, time-
2 series

3

4 1. Introduction

5 Volatile organic iodocarbons (VOIs) such as methyl iodide (CH_3I), chloriodomethane (CH_2ClI)
6 and diiodomethane (CH_2I_2) have a predominantly oceanic source and supply a significant amount
7 of iodine to the atmosphere (see review by Saiz-Lopez and Von Glasow, 2012). These gases, also
8 referred to as VSLS (**very short-lived halogenated substances**) due to their reactivity and short
9 atmospheric lifetimes, have been implicated in supporting catalytic ozone destruction in the
10 troposphere (Davis et al., 1996; McFiggans et al., 2000) and, potentially in the lower stratosphere
11 (Solomon et al., 1994) as well as aerosol formation in the marine boundary layer (McFiggans et
12 al., 2000, 2004; O'Dowd et al., 2002). Recent modelling of atmospheric reactive iodine ($\text{IO}_x = \text{IO}$
13 $+ \text{I}$) as well as experimental studies (Carpenter et al., 2013; Jones et al., 2010; Mahajan et al., 2010)
14 suggest that the supply of volatile organoiodine represents <50% of the total sea-to-air delivery of
15 reactive iodine, with most being supplied in the form of HOI and I_2 . Nevertheless, the potential for
16 localized higher emissions coupled with their relatively long lifetimes (compared to I_2 and HOI)
17 allows the organic compounds to be a significant source of iodine to the free troposphere and even,
18 potentially, to the lower stratosphere in certain regions (Tegtmeier et al., 2013). Further, Mahajan
19 et. al (2012) noted a strong correlation of IO_x and CH_3I suggesting that the sources of CH_3I and
20 the shorter-lived precursors of IO_x are closely related or depend on similar variables.

21 CH_3I is the most abundant VOI species in the atmosphere (Yokouchi et al., 2011) because of its
22 longer lifetime (days) compared to CH_2ClI (hours) and CH_2I_2 (minutes) (Moessinger et al., 1998;
23 Rattigan et al., 1997). However, the total supply of organically-bound iodine to the atmosphere is

1 several times larger than the CH₃I supply alone (Carpenter et al., 2014) with the bulk of the
2 remainder transported in the form of CH₂I₂ and CH₂ClI (additional iodocarbons such as CH₃CH₂I,
3 CH₂BrI and CHI₃ are generally present in much lower concentration). Despite considerable
4 attention on the oceanic distribution and sea-to-air flux of these compounds, in particular CH₃I
5 (Ziska et al., 2013), it is not yet possible to apportion oceanic production of these compounds,
6 unequivocally, to specific mechanisms. Even for CH₃I, controversy remains, for example, as to
7 the relative importance of direct “biological” or “photochemical” production pathways with
8 experimental evidence reported for both, and correlation analysis generally being inconclusive, in
9 part because of the “snapshot” nature of most studies (Stemmler et al., 2014). Comparisons of
10 models to observed distributions have also proven ambiguous, with localized studies suggesting
11 predominance of a biological production pathway (Stemmler et al., 2013) but a global analysis
12 emphasising photochemical production as the dominant mechanism. This diversity of views has
13 been maintained through a variety of experimental studies (Amachi et al., 2001; Brownell et al.,
14 2010; Hughes et al., 2011; Manley and delaCuesta, 1997; Moore and Tokarczyk, 1993; Moore and
15 Zafiriou, 1994; Richter and Wallace, 2004; Shi et al., 2014a; Smythe-Wright et al., 2006).

16 For compounds other than CH₃I, similar uncertainty exists concerning production pathways, but
17 with fewer underlying studies. Laboratory experiments have shown that the presence of dissolved
18 iodide and dissolved organic matter can lead to production of these compounds in the dark
19 (Martino et al., 2009). Fuse et al. (2003) and Martino et al. (2005) observed that CH₂ClI could be
20 produced by photolysis of CH₂I₂ in artificial and natural seawater. However detailed mechanisms
21 and, especially, their relative importance in the field remain unclear.

22 Time-series observation can reveal processes and controlling factors underlying production and
23 loss of iodocarbons in the ocean and provide data for testing hypotheses and/or models. However,

1 only a very few long-term, time series observations of iodocarbons have been reported to date, all
2 from coastal water. Klick (1992) reported 13 months of weekly measurements of CH_2I_2 and
3 CH_2ClI from very shallow (3.5m) water in the Kattegat at the Swedish coast. Orlikowska and
4 Schulz-Bull (2009) reported a year of weekly data for CH_2ClI , CH_2I_2 , CH_3I and $\text{C}_2\text{H}_5\text{I}$ from a
5 nearshore (3m depth) site in the Baltic Sea. Archer et al. (2007) reported a seasonal study of
6 CH_2ClI , CH_2I_2 , CH_3I , $\text{C}_2\text{H}_5\text{I}$, and CH_2BrI measured weekly at 4 depths (0-50m) in the western
7 English Channel from July 2002 to April 2004. Shi et al. (2014b) reported on the seasonal cycle
8 of CH_3I from surface waters of the Kiel Fjord: a shallow (14 m), brackish water body in northern
9 Germany, which was sampled weekly for 2 years. Shimizu et. al (2017) presented a time-series of
10 vertical profiles (0-90m) of CH_2I_2 , CH_2ClI , CH_3I , and $\text{C}_2\text{H}_5\text{I}$ from the centre of Funaka Bay, Japan,
11 which were measured every 2-4 weeks from March 2012 to December 2014.

12 Here, we report weekly observations of CH_3I , CH_2ClI and CH_2I_2 made over the time-period May
13 2015 to December 2017 at 4 depths (0-60m) in Bedford Basin: a coastal fjord on the east coast of
14 Canada. We report seasonal to interannual variability of the observed concentrations at different
15 depths in the water column and compare our results with the other time-series. We report daily
16 average fluxes to the atmosphere and use a simple, time-varying mass-balance model for near-
17 surface waters to estimate production rates and their variability. We discuss the observed
18 variability of both concentrations and production rates in the light of earlier studies, potentially
19 correlated variables and suggested production pathways.

20

21 2. Methods

22 Time-series measurements of VOIs were carried out in the Bedford Basin (44.69 °N, -63.63 °E)
23 near Halifax, Canada. Bedford Basin is an 8 km long, 17 km² fjord with a maximum depth of 71m

1 and a total volume of 500 km³. The Bedford Basin is connected with continental shelf waters of
2 the Atlantic Ocean through “the Narrows” (a ca. 300 m wide and 20 m deep passage (Fig. 1)). The
3 Basin receives freshwater primarily from the Sackville River at its northwestern end, with a total
4 average freshwater input of 5.41 m³ s⁻¹ (Buckley and Winters, 1992). The average near surface
5 salinity within the Basin is 29 which can be compared with salinities of >30 over the adjacent
6 Scotian Shelf. There are only relatively small horizontal gradients of near-surface salinity within
7 the Bedford Basin itself (typically < 2 difference from close to the Sackville River mouth to the
8 Narrows).

9 Time series observations of physical, chemical and biological parameters have been recorded since
10 1992 (Li, 1998). Our halocarbon samples were collected weekly, in the center of the Bedford Basin,
11 at its deepest point (Fig. 1), between May 2015 and January 2018. Samples were collected with
12 10-L Niskin bottles attached to a rosette sampler at 1, 5, 10 and 60 m (10 m samples were collected
13 biweekly from May to September 2015). The upper three water samples covered the majority of
14 the euphotic zone. The 60m water sample was from typically stagnant, near-bottom water which
15 is renewed by vertical mixing events in late winter, and by occasional intrusions of higher-salinity
16 continental shelf water in both summer and winter. Chlorophyll *a* (Chl*a*), dissolved oxygen, and
17 nutrients were measured weekly at the 4 depths as part of the Bedford Basin Monitoring Program
18 (Details can be found in website: [http://www.bio-iob.gc.ca/science/monitoring-monitorage/bbmp-](http://www.bio-iob.gc.ca/science/monitoring-monitorage/bbmp-pobb/bbmp-pobb-en.php)
19 [pobb/bbmp-pobb-en.php](http://www.bio-iob.gc.ca/science/monitoring-monitorage/bbmp-pobb/bbmp-pobb-en.php)). In addition to the Niskin bottle sampling, vertically continuous
20 measurements of temperature, salinity, dissolved oxygen and Chl *a* properties were measured with
21 a CTD mounted on the rosette. Additional information concerning the measurements of supporting
22 physical and biological parameters can be found in the paper by Burt et al. (2013). **Nutrients were**
23 **measured using a Skalar SAN⁺⁺ autoanalyzer, the precisions of NO₂⁻, NO₃⁻ and NH₄⁺ were ± 0.01**

1 $\mu\text{mol L}^{-1}$, $\pm 0.14 \mu\text{mol L}^{-1}$ and $\pm 0.14 \mu\text{mol L}^{-1}$ respectively. Chl *a* concentration was analyzed
2 using a fluorescence technique (Turner Design Model 10 Fluorometer) with the root mean square
3 error (RMSE) being $0.23 \mu\text{g L}^{-1}$. Dissolved oxygen concentrations were determined at 4 depths
4 using Winkler titration with a precision of $\pm 0.5 \mu\text{mol kg}^{-1}$. The resulting between-lab agreement
5 is approaching the specifications for repeat hydrography required by the Global Ocean Observing
6 System
7 ([http://www.gooscean.org/components/com_oe/oe.php?task=download&id=35904&version=2.](http://www.gooscean.org/components/com_oe/oe.php?task=download&id=35904&version=2.0&lang=1&format=1)
8 [0&lang=1&format=1](http://www.gooscean.org/components/com_oe/oe.php?task=download&id=35904&version=2.0&lang=1&format=1)).

9 The concentrations of iodomethane (CH_3I), chloriodomethane (CH_2ClI) and diiodomethane
10 (CH_2I_2) reported here, as well as of a number of other halocarbons (data not shown), were
11 measured using purge & trap gas chromatography with detection by both mass spectrometry (MS)
12 and electron capture (ECD). All measurements were made using an Agilent Technologies gas
13 chromatograph (GC 7890B), equipped with a capillary column (RTX-VGC; 60 m; $1.4 \mu\text{m}$ coating,
14 column diameter: 0.25 mm ; helium carrier gas 0.5 ml min^{-1}), together with an automated purge
15 and trap system equipped with an autosampler (VSP4000 of IMT, Vohenstrauß, Germany). The
16 GC column was temperature programmed as follows: initial temperature $50 \text{ }^\circ\text{C}$ for 6 minutes, then
17 ramped to $150 \text{ }^\circ\text{C}$ at $6 \text{ }^\circ\text{C min}^{-1}$; ramped to $200 \text{ }^\circ\text{C}$ at $10 \text{ }^\circ\text{C min}^{-1}$. Water samples (10 ml) were
18 stored in 20 ml vials equipped with an ultra-low-bleed septum, prior to purging with helium (20
19 ml min^{-1} for 18 mins). Every sample was analysed in triplicate. The standard deviation of triplicate
20 measurements (integrated peak area) was $<10 \%$ for CH_3I , $<15 \%$ for CH_2ClI and $<20 \%$ for CH_2I_2 .
21 Calibration of the GC system for CH_3I , CH_2ClI and CH_2I_2 was performed using permeation tubes
22 (VICI, Houston, TX, USA) which were maintained at a constant temperature of $23 \text{ }^\circ\text{C}$ and weighed
23 every 2 weeks. Dilutions of the permeation tube effluent were made in ultra-high-purity N_2

1 (>99.995 %) with flow rates of 50 to 700 ml min⁻¹, and samples were injected into the purge and
2 trap system (VSP) through a 140 µl loop. Standard deviation of the peak area during these
3 calibration runs was <5 % for CH₃I and CH₂ClI and <15 % for CH₂I₂. Overall the calibration
4 response varied by less than 15 % over the entire sampling period.

5 Throughout the paper, seasons are defined as follows: summer is June through August; fall is
6 September through November; winter is December through February and spring is March to May.

7

8 3. Results and discussion

9 3.1 Environmental Variables from the Bedford Basin

10 The vertical profiles of temperature, salinity, dissolved oxygen and fluorescence (Fig. 2) are well-
11 mixed from top to bottom in late winter (Feb-Mar) as a result of wind-mixing and convection (Li,
12 2001). Temperature is marked by strong seasonality to depths of <30 m. Near-surface temperatures
13 start to rise above winter values of 4 °C, and stratified conditions develop, around early April with
14 temperatures reaching ca. 21 °C by the end of August (Fig. 2a).

15 Salinity ranges from 23 to 31 through the entire water column, with the lowest salinities occurring
16 very close to the surface (Fig. 2b and Fig. 3c). The near-surface stratification varied both seasonally
17 and between years, primarily in association with variability of precipitation and the discharge of
18 the Sackville River (source: Environment and Climate Change Canada;
19 http://climate.weather.gc.ca/historical_data/search_historic_data_e.html). For example, the
20 salinity difference between 1m and 5m was >1 during much of the summer of 2015 (June to
21 September) and summer 2017 (June to August). In summer 2016, however, the salinity at 1m was
22 close to that at 5m (difference < 0.3) (Fig. 3c). Occasional intrusions of more dense water from the
23 Scotian Shelf, results in increased salinity, especially of bottom waters. The intrusions are irregular

1 and tend to occur a few times per year, for instance in May 2016 at which time the salinity of
2 bottom water increased from 30.8 to 31.0 (Fig. 2b), and in early July 2017 when the salinity of
3 mid-depth water increased from 30.5 to 31 (see marked circle in Fig. 2b).

4 The dissolved oxygen time-series (Fig. 2c) shows the effect of temperature-dependent solubility
5 variations in surface waters as well as intrusions and late-winter vertical mixing in deeper water.
6 In surface water the highest O₂ concentrations occurred between March and April every year in
7 association with lowest seawater temperature. The vertical gradient of O₂ concentration was,
8 generally, smallest towards the end of April as a result of vertical mixing. Sub-surface O₂
9 concentrations (>30 m) generally decreased in summer due to respiration, with occasional
10 interruptions of this O₂ decline (e.g. November 2016) as a consequence of shelf-water intrusions
11 which brought sudden increases in O₂ levels.

12 Fig. 3 depicts time-depth plots of the variation of chlorophyll *a*, total dissolved inorganic nitrogen
13 (DIN = [NH₄⁺] + [NO₂⁻] + [NO₃⁻]), salinity, precipitation, windspeed and solar irradiance in
14 Bedford Basin over the period of the VOIs sampling. The seasonal variations of chlorophyll *a*
15 concentration in surface water (Fig. 3a) show that two blooms (spring and autumn) occur in surface
16 water. For example, in 2016, chlorophyll *a* increased rapidly from March to April (from 5 to 26
17 µg L⁻¹), and from September to October (from 10 to 28 µg L⁻¹). The vertical variation of
18 chlorophyll *a* (as determined from fluorescence measured on the CTD, see Fig. 2d) reached 12 µg
19 L⁻¹ during the bloom period. Sub-surface (20- 40 m) fluorescence-derived chlorophyll *a* dropped
20 down to 4 µg L⁻¹. In the near-bottom water chlorophyll *a* ranged between 0 and 2 µg L⁻¹ during
21 the whole year and varied only slightly.

22 The seasonal variation of dissolved inorganic nitrogen(DIN) in surface water is plotted in Fig. 3b.
23 In winter, when chlorophyll *a* levels are very low due to light limitation, DIN concentrations reach

1 ca. $12 \mu\text{mol L}^{-1}$ but are drawn down to low levels ($< 1 \mu\text{mol L}^{-1}$) after the spring bloom.
2 Summertime chlorophyll *a* levels are moderate but variable (ca. 3 to $10 \mu\text{g L}^{-1}$), likely reflecting
3 continuing nutrient input (e.g. from runoff and/or sewage treatment plants). The average
4 precipitation in Bedford Basin was $27.6 \text{ mm week}^{-1}$ in summer 2015 and was 16 mm week^{-1} in
5 summer 2016 (Fig. 3d). Typically, strongest irradiance (data was downloaded from the CERES
6 FLASHFLUX system: <https://power.larc.nasa.gov/cgi-bin/hirestimeser.cgi>) occurs in June and
7 July (see Fig. 3f), and highest water temperatures are observed in August.

8 3.2 Variations of Iodocarbons Concentrations in Bedford Basin

9 Iodocarbon concentrations in surface water (1, 5 and 10 m) showed strong seasonality, with lowest
10 concentrations from December through May (1.2 pmol L^{-1} for CH_3I ; 1.3 pmol L^{-1} for CH_2ClI and
11 0.3 pmol L^{-1} for CH_2I_2). Concentrations start to increase in late May/ June, reaching levels as high
12 as 45 pmol L^{-1} for CH_3I ; 160 pmol L^{-1} for CH_2ClI and ca. 80 pmol L^{-1} for CH_2I_2 (with a single
13 peak of $500.5 \text{ pmol L}^{-1}$; Fig. 4). Near-surface, summertime concentrations of all three compounds
14 were characterized by a broad seasonal peak of 6-7 months duration (or shorter for CH_2I_2), on top
15 of which were superimposed ca. 3-4 peaks of ca. 1 month duration. The number, amplitude and
16 timing of these peaks varied amongst the three compounds with CH_3I , notably, showing only one
17 large peak in 2016 and four during the other two years of the time-series (Fig. 4a).

18 Concentrations at 60 m were almost always lower, and much less variable, ranging over the year
19 from 1 to 9 pmol L^{-1} for CH_3I (except the Fall/Winter 2015-2016, see below), 1 to 6 pmol L^{-1} for
20 CH_2ClI and 0.4 to 18 pmol L^{-1} for CH_2I_2 (Fig. 4d) respectively. Hence, the bottom water (60 m)
21 concentrations of CH_2I_2 and CH_2ClI were always much lower than in near-surface waters
22 throughout the summers. The surface to deep concentration difference was smallest for CH_3I and
23 showed interannual variability. Notably bottom water concentrations reached 26 pmol L^{-1} and were

1 even higher than in contemporary surface waters from September 2015 to March 2016 (Fig. 4d).
2 Missing from the bottom water time-series, were the ca. 1 month duration variations seen in
3 summertime surface water.
4 Inter-relations between the iodocarbons in surface seawater were examined with linear regression
5 of both weekly and monthly-averaged concentrations. The resulting correlations are shown in
6 Table 1. Using weekly data, significant correlations (i.e. $p < 0.05$) were found between [CH₃I] and
7 [CH₂ClI] at 1, 5 and 10 m depths with the strongest correlation ($R = 0.7$) at 10m. The only other
8 significant correlation was between CH₂I₂ and CH₂ClI at 5 m. Use of monthly averaged values
9 gave stronger correlations. Once again, the significant correlations were between CH₃I and CH₂ClI
10 (at 1, 5 and 10m depth) as well as between CH₂ClI and CH₂I₂ at 5 and 10m depth. Table 2 also
11 presents the correlations of iodocarbon concentrations with potentially related variables (discussed
12 in section 4.3).
13 Generally, the concentration of CH₂I₂ was higher than that of CH₂ClI. The average ratio of
14 CH₂I₂/CH₂ClI within the top 10m of the water column over the summer months was 1.4. However,
15 this ratio was significantly lower at 1m depth (average of 0.6) and increased with depth (1.5 at 5
16 m and 2.2 at 10 m, reaching values as high as 2.7 at 60 m).

17

18 3.3 Sea-to-Air Flux

19 Using the concentrations of CH₃I, CH₂ClI and CH₂I₂ at 1m depth (Fig. 4) we estimated the sea-to-
20 air flux of VOIs (F) using the following equation and the parameterization of Nightingale et al.,
21 2000) for the water-side transfer velocity:

$$22 \quad Flux = K(C_{aqu} - C_{air} \times H) \quad (1)$$

$$23 \quad K_w = \left(\frac{Sc}{660}\right)^{-0.5} (0.222 \cdot u_{10}^2 + 0.333 \cdot u_{10}) \quad (2)$$

1 where u_{10} is windspeed at 10 m height, Sc is the temperature-dependent Schmidt number, as
2 estimated by Groszko (1999) and Henry's Law constants (H) were from Moore et al. (1995). The
3 air-side resistance has been shown by Archer et al. (2007) to be significant for soluble gases such
4 as CH_2Cl_2 and CH_2I_2 . Hence K in equation 1 is calculated as follows (Liss and Slater, 1974):

$$5 \quad \frac{1}{K} = \frac{1}{K_w} + \frac{1}{HK_a} \quad (3)$$

6 where the air-side transfer velocity was calculated according to Duce et al. (1991).

$$7 \quad K_a = u_{10}/(770 + 45(MW)^{1/3}) \quad (4)$$

8 with MW being the molecular weight of the gas of interest.

9 Daily averaged wind speed was measured at the nearby Halifax Dockyard (Fig. 1) (source:
10 Environment and Climate Change Canada; http://climate.weather.gc.ca/index_e.html). Seawater
11 temperature and surface iodocarbon concentrations were interpolated linearly between the weekly
12 measurements in order to coincide with the wind speed data and generate daily flux estimates.
13 Following Archer et al. (2007) and Shimizu et al. (2017), we applied an atmospheric concentration
14 of zero for calculating the flux of all three compounds. Rasmussen et al. (1982) reported an average
15 atmospheric mixing ratio of CH_3I of ca. 1 pptv for Cape Meares (45 °N) and Yokouchi et al. (2008)
16 presented a mean concentration of 0.98 pptv for Cape Ochiishi (43.2 °N), with both sites sharing
17 a similar latitude to our sampling location (44.69 °N). If a mixing ratio of 1pptv had been used for
18 our calculations, the total annual flux of CH_3I would be reduced by only 5 %. Atmospheric mixing
19 ratios of CH_2Cl_2 and CH_2I_2 are generally lower (reviewed by Carpenter, 2003) so that any
20 overestimation of the fluxes of these compounds due to this assumption will certainly be negligible
21 (Archer et al., 2007).

22 Fig. 5 presents the weekly averaged combined flux of organically-bound iodine, F_{Iorg} , as stacked
23 bar charts, where $F_{Iorg} = (F_{CH_3I} + F_{CH_2Cl_2} + 2 * F_{CH_2I_2})$. The calculated emissions of individual

1 compounds ranged from 0.9 to 39.2 nmol m⁻² d⁻¹ for CH₃I (annual average of 8.4 nmol m⁻² d⁻¹),
2 0.9 to 78.0 nmol m⁻² d⁻¹ for CH₂ClI (annual average of 17.4 nmol m⁻² d⁻¹) and 0.3 to 78.0 nmol m⁻²
3 d⁻¹ for CH₂I₂ (annual average of 10.3 nmol m⁻² d⁻¹). Seasonal and annual average fluxes of the
4 individual compounds and of I_{org} are presented in Table 3. Clearly the sea-to-air flux is highest in
5 summer and fall and is dominated by the flux of the dihalomethanes rather than CH₃I.

6
7

8 3.4 Net Production of CH₃I

9 We used a mass balance approach to estimate the production rate of CH₃I within the uppermost
10 10m of the water column, based on the concentration time-series (see also Shi et al., 2014b). Using
11 the annual cycle of average near-surface CH₃I concentrations (Fig. 4a), we examined the mass
12 balance of CH₃I for this fixed depth interval according to:

$$13 \quad \Delta C = P_{net} - L_{sea-to-air} - L_{SN2} - L_{mix} \quad (5)$$

14 where ΔC is the daily change of the average CH₃I concentration in the near-surface seawater (0-10
15 m); P_{net} represents the net of gross production minus any additional, uncharacterized losses such
16 as microbial degradation; $L_{sea-to-air}$ is the sea-to-air flux (section 3.3) and L_{SN2} is the ‘chemical’ loss
17 due to nucleophilic substitution of Cl⁻ for I⁻ which was calculated based on reaction kinetics (Elliott
18 and Rowland, 1993; Jones and Carpenter, 2007) using the corresponding temperature, salinity and
19 mean concentration of CH₃I. L_{SN2} averaged 0.1 pmol L⁻¹ day⁻¹. L_{mix} is the loss due to downward
20 mixing and has been shown in several studies to be negligible compared with other loss terms e.g.
21 (Richter and Wallace, 2004). The latter assumption will not always be valid in winter and,
22 especially, when mixed layers deepen to >10m. However most production of iodocarbons occurs
23 during summer and fall when there is strong stratification within the upper 10m (see Fig. 3c), and

1 we excluded from our mass balance calculations the limited periods of time when density was
2 uniform in this depth interval.

3 The net production rate of CH₃I over the 3-year time-series is shown in Fig. 6. The annual average
4 production rate of CH₃I was 1.0 pmol L⁻¹ day⁻¹ (ranging from -1.6 to 8.5 pmol L⁻¹ day⁻¹). A
5 significant peak of P_{net} occurred from August to September in every year. The net production rate
6 of CH₃I in summer and fall averaged 1.6 pmol L⁻¹ day⁻¹ and was 5 times larger than wintertime
7 rates (ca. 0.3 pmol L⁻¹ day⁻¹). Net production rates for CH₂ICl and CH₂I₂ were also calculated
8 (results not shown), with typical summertime values being 3.2 and 1.3 pmol L⁻¹ day⁻¹, respectively.
9 Photolytic loss can be very significant for these compounds and has not been estimated, so these
10 P_{net} values represent the net of gross production minus uncharacterized losses including photolysis
11 as well as microbial degradation.

12

13 4. Discussion

14 In the following we discuss the Bedford Basin data in comparison with other studies that have
15 reported concentrations of multiple iodocarbons and especially those that have reported time-series
16 covering an annual cycle (see citations in the introduction). All of these time-series are from mid-
17 latitude (40-60°N) nearshore or continental shelf environments subject to strong seasonal
18 variations of light, temperature and biological productivity. There are no reported time-series of
19 seawater concentrations from low latitudes.

20

21 4.1 Potential influence of nearshore and /or macroalgal sources

22 The potential of nearshore macroalgae to cause elevated coastal iodocarbon concentrations has
23 been mentioned in a number of studies (Giese et al., 1999; Manley and delaCuesta, 1997; Schall

1 et al., 1994). We investigated this in July 2017, by sampling at 5 nearshore sites around Bedford
2 Basin (Fig. 1) and comparing nearshore concentrations with values measured at the regular
3 sampling site in the center of the Basin (Table 4). The nearshore results were consistently within
4 one standard deviation of mean concentrations of VOIs measured at the center of Bedford Basin
5 during July, indicating no significant difference. Klick (1992) also compared measurements on
6 samples collected directly over a rich bed of macroalgae with samples collected further away from
7 direct contact with macroalgae: whereas they observed significantly higher concentrations of
8 bromocarbons in proximity to the macroalgae, there was no difference observed for CH_2I_2 and
9 CH_2ClI . Shimizu et al. (2017) sampled a number of nearshore regions around Funka Bay, including
10 rocky shores with extensive macroalgae, and also found concentrations to be similar at both
11 nearshore and central Bay locations. We therefore conclude that any direct impact of macroalgae
12 on measured organoiodine levels is small, even in coastal regions, which lends strong support to
13 the conclusion by Saiz-Lopez and Von Glasow (2012) that macroalgae are only a minor global
14 source of these compounds to the atmosphere.

15

16 4.2 Concentrations and relative abundance of iodocarbon compounds

17 The average concentration of total volatile organic iodine I_{org} (where $I_{\text{org}} = [\text{CH}_3\text{I}] + [\text{CH}_2\text{ClI}] +$
18 $2[\text{CH}_2\text{I}_2]$) and the relative contributions of the different compounds to I_{org} from this and other
19 studies is shown in Fig. 7. The combined concentrations of the three iodocarbons are highest but
20 also show highest variability ($[I_{\text{org}}] = 25$ to 281 pmol L^{-1}) in summertime coastal waters (loosely
21 defined here as within a few kms of land). Continental shelf waters have lower concentrations of
22 I_{org} averaging 32 pmol L^{-1} , with open ocean waters having comparable or lower concentrations
23 (average $I_{\text{org}} = 17 \text{ pmol L}^{-1}$). Despite the differences in I_{org} concentration ranges evident for

1 different regions in Fig. 7, a 1-way ANOVA showed no significant differences between the means
2 for the three regions. However after pooling of shelf and open ocean results to make only two
3 populations, a t-test did reveal a significant difference with coastal waters for at the 95%
4 confidence level.

5 The distribution of I_{org} is contrary to the global distribution of CH_3I reported by Ziska et al. (2013)
6 who noted a tendency for the open ocean to have higher concentrations than coastal waters (their
7 definition of “coastal” was within 1 degree latitude or longitude of land and therefore much broader
8 than ours). As noted by Ziska et al. (2013), this may reflect higher CH_3I concentrations in tropical
9 and sub-tropical open ocean waters, as their general pattern was reversed in the Northern
10 Hemisphere. The coastal waters depicted in Fig. 7 are largely from mid-latitudes of the Northern
11 Hemisphere.

12 The relative contribution of the dihalomethanes to I_{org} also appears to vary between regions, with
13 the ratio of dihalomethane-I to I_{org} , $([\text{CH}_2\text{CII}] + 2 * [\text{CH}_2\text{I}_2]) / [I_{\text{org}}]$, averaging 0.71, 0.69 and 0.55 in
14 coastal, shelf and open ocean waters, respectively. While an elevated contribution of
15 dihalomethanes in coastal waters is consistent with the report by Jones et al. (2010), regional
16 differences apparent in Fig. 7 are not significant at the 95% confidence level when tested with a 1-
17 way ANOVA.

18 Klick (1992), Jones et al. (2010) and Shimizu et al. (2017) reported concentrations of volatile
19 organic iodine in summertime coastal waters that are comparable to, or higher than those observed
20 in Bedford Basin (i.e. average I_{org} concentrations $> 100 \text{ pmol L}^{-1}$). Our results from Bedford Basin
21 correspond closely with concentrations and relative contributions reported by Shimizu et al. (2017)
22 for coastal water in Funka Bay, Japan (Fig. 7). In these coastal surface waters, the CH_2I_2
23 concentration and contribution was highest on average, followed by CH_2CII and the lowest was

1 CH₃I. In open ocean waters, the relative contribution of [CH₃I] to I_{org} appears higher, reaching
2 over 50% in some cases (see Fig. 7), with the contribution of CH₂I₂ generally being lower in the
3 open ocean than in coastal waters. However, once again, these apparent regional differences are
4 not significant at the 95% confidence level.

5 In laboratory studies, Fuse et al. (2003) demonstrated that relatively large amounts of CH₂I₂ and
6 I₂ together with smaller but still significant amounts of CH₂ClI and CHI₃ can be produced,
7 presumably abiotically, in dark incubations of (filtered) spent culture media with suspended
8 bacterial cells and added [I⁻]. The CH₂I₂/CH₂ClI production ratio was ~35 and no mono-iodinated
9 CH₃I was produced in these experiments. The implication was that dissolved organic compounds
10 within spent media were key to production of polyiodinated compounds. In the absence of spent
11 culture media, additions of oxaloacetic acid also resulted in formation of CH₂I₂ and CH₂ClI (with
12 a lower ratio of CH₂I₂/CH₂ClI of ~10) suggesting that organic acids may be a substrate for their
13 formation. The mechanistic role of the suspended bacterial cells was not clear, however they may
14 have supplied haloperoxidases required for oxidation of I⁻ (see also Hill and Manley, 2009).
15 Martino et. al (2009) demonstrated that, alternatively, oxidation of dissolved iodide to I₂ and HOI
16 by reaction with ozone (e.g. Garland et al., 1980) in filtered (0.2 μm) seawater containing natural
17 levels of dissolved organic matter also resulted in formation of polyiodinated compounds (CH₂I₂,
18 CH₂ClI and CHI₃) with CH₂I₂/CH₂ClI production ratios ranging from 2 to 4. They suggested that
19 the yield of various iodocarbons depends on “the abundance and perhaps on the nature of the
20 organic substrate” which “can vary widely both temporally and spatially”. We could not, however,
21 find any obvious relationship of near-surface iodocarbon concentrations with local measurements
22 of atmospheric ozone near Bedford Basin (results not shown).

1 We therefore suggest that the higher levels of CH_2I_2 observed in coastal waters, including Bedford
2 Basin, reflect a higher supply rate of HOI and/or I_2 and/or of the organic precursors suitable for
3 formation of polyiodinated compounds. Ultimately, reduction of seawater iodate to reduced forms,
4 such as iodide, likely supports the potential for organoiodine formation. Addition of iodide has
5 been identified, in short-term experiments, as a source for reactive iodine (iodine atoms) which
6 can stimulate photochemical formation of CH_3I (Moore and Zafiriou, 1994). However, Shi et. al
7 (2014b) found no positive correlation of $[\text{I}^-]$ with seasonal CH_3I production in a field study in Kiel
8 fjord, noting that background iodide levels may have been always sufficient to support production
9 of pM levels of CH_3I . Indeed, there is no *a priori* reason to expect a positive correlation of $[\text{I}^-]$ with
10 iodocarbon production if supply of more reactive iodine species (iodine atoms, HOI and/or I_2) is
11 the key, proximate control. The short-term formation rate of reactive species from a background
12 reservoir of I^- , and hence production of iodocarbons, may depend more on availability of
13 haloperoxidases, various oxidants and/or temperature-dependent kinetics. The conversion of I^- to
14 these reactive species could even lead to inverse correlations between I^- and iodocarbons.

15 Relatively small quantities of CH_2ClI were produced in several of the experiments cited above,
16 yet observations in Bedford Basin show average $\text{CH}_2\text{I}_2/\text{CH}_2\text{ClI}$ ratios of 1.4 in the top 10 m of the
17 water column. Production ratios in these experiments vary, as noted above, but laboratory studies
18 have also shown that photolysis of CH_2I_2 can be an important source of CH_2ClI in surface waters
19 with a yield of 25 % to 35 % (Jones and Carpenter, 2005; Martino et al., 2005). We observed
20 significant correlation between $[\text{CH}_2\text{I}_2]$ and $[\text{CH}_2\text{ClI}]$ at 5 and 10 m depth (but not at 1m) (Table
21 1), which is consistent with a fraction of the CH_2I_2 production being transformed photochemically
22 (The lack of correlation at 1m may be due to the very rapid photolysis). However the correlation
23 may also reflect the original production ratio of the individual compounds (which laboratory

1 experiments suggest may be substrate-dependent). In both cases however, dissolved organic matter
2 (DOM) quality and quantity (possibly associated with terrestrial supply) and/or elevated supply of
3 I are likely to be underlying reason(s) for the high concentrations of dihalomethanes observed in
4 Bedford Basin and other coastal waters.

5

6 4.3 Temporal variations of iodocarbons in near-surface water

7 The following discussion of temporal variability is separated into consideration of seasonal and
8 interannual variations.

9 4.3.1 Seasonal Variations

10 All of the reported iodocarbon time-series showed strong seasonality, with minimum, sometimes
11 undetectable concentrations in winter, and higher concentrations in summer. Near-surface (0-10
12 m) concentrations of all three iodocarbons in Bedford Basin, including CH₃I, remained low until
13 mid-May to mid-June, with their subsequent increase coincident with initial warming of near-
14 surface waters from wintertime minimum temperatures of ca. 1-2 °C (lag < 1 month; Fig. 8a).
15 Hence the initial appearance of all three iodocarbons occurred more than 3 months after the
16 seasonal increase in solar radiation, ca. 1-2 months after the Spring Bloom (Fig. 8d), after near-
17 surface nitrate had been drawn down to low levels (Fig. 8e) and almost coincident with the seasonal
18 temperature increase (Fig. 8a).

19 In the western English Channel (Archer et al., 2007), a gradual increase of CH₃I commenced in
20 February, coincident with the seasonal increase in solar radiation. Summertime values remained
21 high, with some higher-frequency variation, and then decreased in September/October. The
22 increase of CH₂ClI and CH₂I₂ started later, in April, more or less coincident with both the Spring
23 Bloom and initiation of near-surface warming from a wintertime minimum temperature of ca. 8

1 °C. Summertime values of CH₂ClI and CH₂I₂ showed periodic variations similar to those observed
2 in Bedford Basin (section 3.2).

3 The lower temporal resolution of the study in Funka Bay (Shimizu et al., 2017), with sampling
4 only every 1 or 2 months, precluded detailed examination of timing. A gradual increase in CH₃I
5 appeared to start in March, during or towards the end of the Spring Bloom when surface water
6 temperatures were still close to their wintertime minimum of -1 to 2.5 °C. The seasonal increase
7 of CH₂I₂ and CH₂ClI occurred later (May-June) at a time of rising water temperatures and low
8 nutrient levels with concentrations remaining elevated through the summer and decreasing to
9 wintertime levels in October.

10 The initial CH₃I increase at a shallow station in the Kiel Fjord (Shi et al., 2014b) occurred in March,
11 and was closely linked in time to seasonal increases of solar radiation, temperature (winter
12 minimum of 0 °C) as well as Chl *a* and the springtime drawdown of nitrate. Lagged correlation
13 analysis showed similarly strong correlations of CH₃I with both temperature and solar radiation,
14 with the annual cycle of CH₃I lagging temperature by ca. 1 month, however the very close
15 correspondence of multiple seasonal cycles led the authors to note that “the use of correlation
16 analysis to infer causality has likely reached its limit in this analysis”.

17 The observation of a rapid increase in the production rate of I⁻ within phytoplankton cultures
18 (diatoms and prymnesiophytes) when they enter stationary and, especially, senescent phases
19 (Bluhm et al., 2011) is potentially relevant to the observed seasonality of iodocarbon formation.

20 The reduction of iodate to iodide was suggested to be due to release of precursors, such as reduced
21 sulphur species, to surrounding culture medium in association with a loss of membrane integrity
22 by stressed cells or as a result of viral lysis. Hughes et al. (2011) also reported studies with cultures
23 of *Prochlorococcus marinas* in which accumulation of CH₃I commenced when cultures became

1 senescent. We note that significant iodocarbon accumulation in Bedford Basin was confined to
2 summertime when DIN was depleted (see Fig. 3b) and when cells may have been stressed or
3 subject to viral lysis, perhaps similar to later stages of batch culture experiments.

4 We therefore hypothesize that seasonal nitrate drawdown leads to increased supply of iodide to
5 surface waters which can, in turn, lead to increased formation of iodine atoms, HOI and I₂ as
6 precursors for iodocarbon formation by both photochemical and haloform reaction pathways
7 (Martino et al., 2009; Moore and Zafiriou, 1994). Whereas the supply of iodide may be one key
8 control, it is likely that variations in light intensity and water temperature also contribute to the
9 overall seasonality of the production rate of CH₃I (e.g. through temperature influence on reaction
10 kinetics). For example, light can influence formation of CH₃I directly (e.g. Moore and Zafiriou,
11 1994; Richter and Wallace, 2004). Light can also influence iodocarbon production indirectly, for
12 example by producing oxidants such as H₂O₂ to promote oxidation of iodide by haloperoxidases
13 (Hill and Manley, 2009) or by altering the quality of dissolved organic matter. The time-series of
14 CH₂I₂ and CH₂ClI from very shallow (< 4 m), nearshore waters of the Kattegat, Sweden (Klick,
15 1992) and the Baltic Sea, Germany (Orlikowska and Schulz-Bull, 2009) showed peaks in April/
16 May and again in September/October, with low concentrations throughout summer. This contrasts
17 with the deeper water columns of Bedford Basin, Funka Bay and the English Channel where
18 concentrations remain elevated throughout summer. This likely reflects dominance of photolytic
19 loss over production within very shallow water columns exposed to summertime light intensities
20 and long periods of daylight. Sub-surface production coupled with vertical mixing may explain
21 the summertime persistence in deeper water columns.

22 In addition to the broad seasonal variation, a number of maxima with duration of ca. 1 month, were
23 observed, and appear similar to short-period fluctuations observed in the English Channel time-

1 series (Archer et al., 2007). There does not appear to be any consistent pattern linking the maxima
2 and minima of the three compounds in the two studies, so that the underlying causes for these
3 shorter period variations are unclear.

4

5 4.3.2 Interannual variability

6 The Bedford Basin time-series is unique in having high temporal resolution sampling (weekly)
7 over three annual cycles which allows interannual variability to be examined for the first time. The
8 most obvious interannual difference was in the behavior of CH₃I. In particular, 2016 was markedly
9 different in that only a single peak was observed in late August, whereas the summers of 2015 and
10 2017 were marked by 3-4 quasi-periodic, multi-week maxima. As noted already, the English
11 Channel time-series of CH₃I did not exhibit this behavior. The shallow-water time-series of CH₃I
12 in the Kiel Fjord and coastal Baltic Sea (Orlikowska and Schulz-Bull, 2009; Shi et al., 2014b) also
13 did not exhibit this type of variability. Because the cause of the periodicity itself is not understood
14 or explained, discussion of reasons for its interannual variation must be highly speculative. One
15 clear difference of 2016 relative to the other two years, was the lower summertime precipitation
16 and associated lack of near-surface salinity stratification. The temporal behavior of CH₃I in 2016
17 might therefore be related to altered near-surface mixing dynamics within Bedford Basin, or
18 alternatively, to decreased delivery of key precursors (e.g. DOM) from land via rivers and
19 wastewater.

20

21 4.4 Vertical distributions and subsurface temporal variability

22 Fig. 4 shows the near-surface concentration variations of the VOIs. For CH₃I, concentrations were
23 almost always uniform between 1, 5 and 10 m. For CH₂Cl₂, the concentrations at 1 and 5m were

1 usually very similar (average difference -4.1 %; median -2.5 %), however concentrations at 10m
2 depth were noticeably lower for periods of time. For CH₂I₂, the highest concentrations were
3 observed at a depth of either 5 or 10 m, with concentrations at 5 m occasionally peaking at very
4 high levels (e.g. 250-350 pmol L⁻¹) for short periods (less than one week). Concentrations at 1 m
5 were almost always lower than at 5 m, with the percentage reduction relative to 5 m averaging 52 %
6 in summer. Concentrations at 10 m, on the other hand, were generally the same or higher as those
7 measured at 5 m (with the exception of the previously mentioned, short-lived peaks).
8 These results are consistent with earlier studies of vertical profiles in the open ocean (e.g. Moore
9 and Tokarczyk, 1993; Yamamoto et al., 2001) as well as with model predictions (Jones et al., 2010;
10 Martino et al., 2006). In particular, our results are consistent with the quantitative predictions of a
11 mixed-layer model (Jones et al., 2010) that CH₂ClI would typically be near-uniform within the
12 upper 6 m of the water column, whereas photolytic decay could remove up to 100 % of the CH₂I₂
13 over that depth range, depending on time of day and conditions.

14

15 4.5 Temporal variability in near-bottom water (60 m)

16 The time-series of VOIs in near-bottom waters (60 m) are presented in detail in Fig. 9a,b,c, with
17 specific events labelled 1 through 9. Variability was generally of lower amplitude than in surface
18 waters, except for CH₃I during the winter of 2015-2016 (Fig. 4d). From June to December 2015,
19 [CH₃I] increased steadily (concentration change, $\Delta C = 20$ pmol L⁻¹) (event 1 to 3; Fig. 9a),
20 exceeding surface water concentrations from October 2015 until the end of March 2016. No
21 comparable increase was observed during 2016 (Fig. 9b), and a smaller increase ($\Delta C = 8$ pmol L⁻¹)
22 was confined to the early summer of 2017 (Fig. 9c).

1 Concentrations of CH₂ClI remained almost constant at <5 pmol L⁻¹ throughout, with the notable
2 exception of abrupt (<1 week) increases in May and November 2016 (events 4 and 5; Fig. 9b) and
3 December 2017 (event 9; Fig. 9c). These increases ($\Delta C = 2\text{-}5 \text{ pmol L}^{-1}$) coincided with sudden
4 increases of salinity (and O₂) and reflect intrusion of saltier, near-surface waters from offshore,
5 rather than local production. The subsequent concentration declines reflect loss due to mixing or,
6 more likely, reaction and/or microbial degradation within the water column and sediments. The
7 same three intrusions also drove abrupt increases of CH₂I₂ with amplitude ca. 1.5 – 2 times higher
8 than those for CH₂ClI, consistent with near-surface concentration ratios (see section 3.2). However,
9 CH₂I₂ also showed higher-amplitude variations unrelated to the bottom water intrusions (see
10 below).

11 The increase of CH₃I from June through October 2015 (event 1 through 3; Fig. 9a), paralleled a
12 steady decline in oxygen, suggesting that production was linked to degradation of organic matter.

13 The accumulation rate of ca. 0.06 pmol L⁻¹ day⁻¹ was 20 times smaller than typical P_{net} for CH₃I
14 in surface waters (see section 3.4). The increase appears consistent with results from short-term
15 (3-day) incubation experiments with biogenic marine aggregates reported by Hughes et al. (2008)
16 in which concentrations of mono-iodinated iodocarbons, including CH₃I, increased but with no
17 corresponding increase in dihalogenated compounds. Their results suggested alkylation of
18 inorganic iodine or breakdown of higher molecular mass organohalogenes as production pathways
19 and, following Amachi et al. (2001), they suggested that microbial degradation increased the
20 supply of precursors.

21 However, as O₂ concentrations declined further from October through late December (event 2 to
22 3; Fig. 9a), the concentration of CH₃I stabilized and CH₂I₂ concentration increased markedly from
23 2 to 12 pmol L⁻¹. From January through April 2016, CH₃I levels decreased (following event 3; Fig.

1 9a,b), in concert with increasing O₂ concentrations and decreasing salinity, reflecting the effects
2 of progressive vertical mixing with overlying waters which had lower CH₃I concentrations. Over
3 this same period, CH₂I₂ concentrations at 60 m remained almost constant (Fig. 9a, b) due to the
4 smaller vertical concentration gradient, until increasing due to an intrusion (event 4). This was
5 followed by a gradual decrease over summer months, in parallel with the seasonal decrease of O₂
6 (fig 9b).

7 The data from 2015 and 2017 are suggestive of a “switch” of production mechanism from an
8 alkylation pathway producing mono-iodinated compounds (CH₃I) to a haloform-type reaction
9 producing CH₂I₂. The “switch” took place in October 2015 (event 2; Fig. 9a), when oxygen
10 concentrations dropped below 90 μmol kg⁻¹, although whether the switch was related to redox
11 conditions in the water column or sediments, speciation and availability of iodine, or availability
12 of suitable organic precursors and/or enzymes cannot be determined.

13 There was almost no near-bottom iodocarbon production during 2016 (Fig. 9b), and therefore no
14 “switch”, for reasons that are not clear given that O₂ declined through summer and fall, until
15 interrupted by an intrusion in November (event 5; Fig. 9b). We speculate that the lack of production
16 in near-bottom water might be linked to the relatively short period of CH₃I production in near-
17 surface waters during that year (fig 4a).

18 In 2017, there was moderate sub-surface production of CH₃I, associated with O₂ consumption
19 (April through July; event 6 to 7), and, again, an apparent “switch” to CH₂I₂ production marked
20 by plateauing of CH₃I concentrations (event 7) at the same time as CH₂I₂ concentrations started to
21 increase (Fig. 9c). This was followed by a subsequent decrease to background levels over a period
22 of about a month. The apparent “switch” in production took place earlier in the year and at higher
23 O₂ concentrations (175 μmol kg⁻¹) than in 2015.

1 However close inspection of Fig. 2 shows that the plateauing of CH₃I in near-bottom waters (event
2 7) also coincided with the appearance of a mid-depth intrusion of saltier water (as denoted by the
3 31 salinity contour; see blue circled area in Fig. 2). The same period (between events 7 and 8) was
4 marked at 60m by a change from declining to increasing salinity, reduction in the rate of oxygen
5 concentration decline (Fig. 9c) and an increase in the rate of warming (not shown). The mid-depth
6 salinity maximum in Bedford Basin must reflect intrusion of saltier water from offshore. The
7 subsequent trends in temperature, salinity and dissolved oxygen at 60m, between events 7 and 8
8 (Fig. 9c), are consistent with mixing of pre-existing near-bottom water with this intrusion. It
9 therefore cannot be ruled out that mixing with this intrusion contributed in some way to the near-
10 bottom increase of CH₂I₂, plateauing of CH₃I concentrations as well as the small but significant
11 increase in CH₂ClI ($\Delta C=1-2$ pmol L⁻¹), and hence to the apparent “switch”, which all occurred at
12 the same time.

13 At the end of this period, in mid-August (event 8), the rate of warming and salinity increase at 60
14 m decreased again and the rate of oxygen decline increased (Fig. 9c), suggesting that the
15 intrusion’s impact had lessened. At this time, CH₂I₂ and CH₃I concentrations started to return to
16 background levels with estimated half-life, assuming 1st order kinetics, of ca. 65 days (CH₂I₂) and
17 14 days (CH₃I). A decrease in [CH₂ClI] started about a month later with 1st order half-life of ca.
18 70 days. Similar rates of decline of [CH₂ClI] and [CH₂I₂] were observed following sudden
19 concentration increases associated with other intrusions, discussed earlier.

20 This very detailed discussion of the temporal variability emphasizes that a variety of physical and
21 biogeochemical mechanisms can contribute to interannual, seasonal, and short-term variability of
22 the three iodocarbons. The high amplitude variability observed in Bedford Basin could prove
23 useful for validation of models representing complex iodine cycling as well as physical mixing

1 dynamics. However, separation of multiple potential contributing factors and processes underlying
2 temporal variability may require a data set with higher vertical resolution and, ideally, a seasonally-
3 resolved time-series of experiments (compare Shi et al., 2014a).

4

5 4.6 Sea-to-air fluxes

6 The temporal variation of the sea-to-air flux of I_{org} and the relative contribution from the three
7 iodocarbons are shown in Fig. 5 and Table 3. Similar to the findings of Archer et al. (2007), air-
8 side resistance leads to significant reductions in calculated, annual average fluxes for CH_2ClI and
9 CH_2I_2 of 10% and 24%, respectively, relative to calculations when it is ignored. The study by
10 Shimizu et al. (2017) did not consider air-side resistance, so Table 5 presents both their original
11 reported fluxes, as well as fluxes adjusted for its likely impact based on our study and that of
12 Archer et al. (2007). The following discussion makes use of the adjusted fluxes.

13 Consistent with earlier time-series (excluding those from very shallow waters, see section 4.2), the
14 sea-to-air flux of iodocarbons is generally highest in summer/fall. However, high wintertime fluxes
15 are also possible, as seen in 2017 when there was a large efflux of CH_2I_2 (averaging 9.1 nmol m^{-2}
16 d^{-1} ; Table 3), due to both strong winds and relatively high concentrations. The fluxes of CH_3I and
17 CH_2ClI , on the other hand, were always higher in summer/fall (ca. 3-5 times and 10 times higher,
18 respectively). Similar findings were presented by Shimizu et al. (2017) with the total iodine flux
19 in Funka Bay in summer being > 4 times that in winter.

20 Our estimated emissions of CH_3I ($8.4 \text{ nmol m}^{-2} \text{ d}^{-1}$, Table 5) are in the range calculated previously
21 for coastal and continental shelf water in similar latitudes (11.9 and $7.7 \text{ nmol m}^{-2} \text{ d}^{-1}$; Archer et
22 al., 2007; Shimizu et al., 2017 respectively). The average flux of CH_3I reported by Jones et. al
23 (2010), from the west of Ireland, was 4 times higher but based on a sampling period of only 1

1 month during summer. Sea-to-air fluxes of CH_2ClI from Funka Bay and English Channel were similar to our calculated fluxes from Bedford Basin. However the highest variation is observed in the annual averaged flux of CH_2I_2 , ranging from $3.5 \text{ nmol m}^{-2} \text{ d}^{-1}$ (the west English Channel), $10.3 \text{ nmol m}^{-2} \text{ d}^{-1}$ (Bedford Basin) and $12.6 \text{ nmol m}^{-2} \text{ d}^{-1}$ (Funka Bay, Japan). The total, annual I_{org} sea-to-air flux from Bedford Basin averaged $46.7 \text{ nmol m}^{-2} \text{ d}^{-1}$, which was approximately 5 times larger than the flux due to CH_3I alone. The total annual flux was similar between all three locations. Fig. 5 and Table 3 show that the total I_{org} flux is subject to significant interannual variability, which could not be assessed by the earlier studies. Notably, the I_{org} flux in 2016 was ca. 2 times smaller than in 2015 and 2017. A comparison of wind-speeds and concentrations showed that the influence of wind speed was dominant, due to winds during summer/fall of 2016 being $1\text{-}2 \text{ m s}^{-1}$ lower.

4.7 Production rate of CH_3I

The annual mean production rate (P_{net}) of CH_3I in this study, estimated using equation 1, was $1.0 \text{ pmol L}^{-1} \text{ day}^{-1}$ (ranging from -1.6 to $8.5 \text{ pmol L}^{-1} \text{ day}^{-1}$, see section 3.4 and Fig. 6). This is comparable with the global average production rate estimated by Stemmler et al. (2013) ($1.64 \text{ pmol L}^{-1} \text{ day}^{-1}$), for which 70% was produced via a photochemical mechanism. Based on data presented by Archer et al. (2007), the annual mean production rate of CH_3I in the western English Channel was ca. $2 \text{ pmol L}^{-1} \text{ day}^{-1}$ (range: -0.2 to $6 \text{ pmol L}^{-1} \text{ day}^{-1}$). Here it should be noted, that their “minimum gross production rate” is equivalent to P_{net} in this study and in Shi et al. (2014a). In contrast, Shi et al. (2014b) estimated a considerably lower annual mean net production rate in the Kiel Fjord of ca. $0.1 \text{ pmol L}^{-1} \text{ day}^{-1}$ (maximum of $0.8 \text{ pmol L}^{-1} \text{ day}^{-1}$). The maximum production rates from the Kiel Fjord study were smaller as they were based on monthly average (and therefore “smoothed”) concentrations. However, Shi et al. (2014a) also conducted weekly incubation

1 experiments which gave *in vitro* values of P_{net} which were closely comparable with the field-based
2 estimates in Kiel Fjord.

3 The lower values of P_{net} in the Kiel Fjord compared with both Bedford Basin and the English
4 Channel must reflect either differences in gross production (e.g. due to differences in the supply
5 of precursors and reactants such as iodide) or differences in other, uncharacterized losses. Evidence
6 for a poorly characterized loss process, possibly microbial degradation, was in fact observed in the
7 Kiel Fjord incubation experiments (Shi et al., 2014a). On the other hand, incubation experiments
8 conducted with additions of labelled methyl iodide ($^{13}\text{CD}_3\text{I}$) to Bedford Basin surface waters (data
9 not shown) during the course of this study showed no such losses. We therefore hypothesize that
10 the lower P_{net} in Kiel Fjord is a result of higher microbial degradation of CH_3I in that very shallow
11 (<12 m), nearshore environment.

12

13 5. Conclusions, Implications and Further Work

14 The 3-year time-series of weekly iodocarbon concentrations from Bedford Basin shows overall
15 seasonality similar to that observed in coastal time-series from both the English Channel and Funka
16 Bay, Japan. There was no mid-summer minimum in the concentration of polyiodinated compounds
17 as observed in some time-series from very shallow water (<10m), which likely reflects dominance
18 of photolytic decay in such shallow water columns. Interannual variability in near-surface water
19 concentrations was particularly pronounced for CH_3I , with only a single, short-lived concentration
20 maximum observed in 2016, possibly as a result of anomalously low rainfall and consequently
21 reduced supply of terrestrial organic matter during that summer.

22 Based on the time-series as well as published lab studies, we hypothesize that seasonal, near-
23 surface production of iodocarbons is linked to accelerated reduction of iodate to iodide under post-

1 bloom conditions, following disappearance of nutrients and possibly also influenced by water
2 temperature. The observed vertical variation of CH_2I_2 and CH_2ClI is consistent with the more rapid
3 photolysis of CH_2I_2 .

4 The average annual sea-to-air flux of total volatile organic iodine ($46.7 \text{ nmol m}^{-2} \text{ d}^{-1}$) is almost
5 identical to that observed in Funka Bay, Japan, and the English Channel. The polyiodinated
6 compounds contributed ca. 80 % of the total flux which was similar to that in the other two time-
7 series and confirms that the sea-to-air flux of polyiodinated compounds dominates in coastal
8 waters. The fluxes were variable on interannual timescales (factor of 2) as a result, mainly, of
9 wind-speed variability.

10 The near-bottom water (60m) time-series was impacted by episodic intrusions of water from
11 offshore and showed evidence for CH_3I production associated with decay of organic matter, albeit
12 with a production rate more than an order of magnitude lower than in surface waters. The time-
13 series showed evidence for a possible “switch” from CH_3I production (e.g. by alkylation of organic
14 matter) to production of CH_2I_2 (e.g. by a haloform type reaction), after periods of about 1 month.

15 The very high amplitude concentration variations encountered in Bedford Basin, coupled with its
16 relative accessibility for high-frequency sampling and constrained, yet variable, physical
17 exchanges make Bedford Basin a useful location to investigate iodine cycling. To-date, the
18 complexity of iodine biogeochemistry has hindered progress towards understanding the controls
19 on spatial and temporal fluxes of iodine between the ocean and atmosphere. We suggest that
20 progress can now be made through more comprehensive sampling (higher vertical resolution and
21 inclusion of inorganic iodine speciation measurement), coupled to a biogeochemical model of
22 Bedford Basin that includes iodine chemistry (e.g. Stemmler et al, 2013) and a time-series of
23 experimental studies conducted in the context of the time-series (see Shi et al., 2014a). In other

1 words, Bedford Basin may provide an ideal location and time-series upon which to base a multi-
2 investigator campaign to understand environmental controls on volatile iodine cycling and
3 improve its representation in models.

4

5 Acknowledgments

6 This work was funded by the Canada Excellence Research Chair in Ocean Science and Technology
7 at Dalhousie University. Sampling of the Bedford Basin time-series was supported by MEOPAR
8 Observation Core, Department of Fisheries and Ocean, Canada (DFO) and Bedford Basin
9 Monitoring Program (BBMP) ([http://www.bio.gc.ca/science/monitoring-monitorage/bbmp-
10 pobb/bbmp-pobb-en.php](http://www.bio.gc.ca/science/monitoring-monitorage/bbmp-pobb/bbmp-pobb-en.php)). The authors thank Richard Davis, Anna Haverstock and the crew of the
11 Sigma-T. Assistance and guidance in the laboratory from Claire Normandeau and Liz Kerrigan
12 are also acknowledged.

13

14 Reference

15 Amachi, S., Kamagata, Y., Kanagawa, T. and Muramatsu, Y.: Bacteria mediate methylation of
16 iodine in marine and terrestrial environments, *Applied and environmental microbiology*,
17 67(6), 2718–2722, 2001.

18 Archer, S. D., Goldson, L. E., Liddicoat, M. I., Cummings, D. G. and Nightingale, P. D.: Marked
19 seasonality in the concentrations and sea-to-air flux of volatile iodocarbon compounds in
20 the western English Channel, *Journal of Geophysical Research: Oceans*, 112(C8), C08009,
21 doi:10.1029/2006JC003963, 2007.

22 Bluhm, K., Croot, P. L., Huhn, O., Rohardt, G. and Lochte, K.: Distribution of iodide and iodate in
23 the Atlantic sector of the southern ocean during austral summer, *Deep Sea Research Part*

1 II: Topical Studies in Oceanography, 58(25), 2733–2748, 2011.

2 Brownell, D. K., Moore, R. M. and Cullen, J. J.: Production of methyl halides by Prochlorococcus
3 and Synechococcus, *Global Biogeochemical Cycles*, 24(2), GB2002, 2010.

4 Buckley, D. E. and Winters, G. V: Geochemical characteristics of contaminated surficial sediments
5 in Halifax Harbour: impact of waste discharge, *Canadian Journal of Earth Sciences*, 29(12),
6 2617–2639, 1992.

7 Burt, W. J., Thomas, H., Fennel, K. and Horne, E.: Sediment-water column fluxes of carbon,
8 oxygen and nutrients in Bedford Basin, Nova Scotia, inferred from ²²⁴Ra measurements,
9 *Biogeosciences*, 10(1), 53–66, doi:10.5194/bg-10-53-2013, 2013.

10 Carpenter, L. J.: Iodine in the marine boundary layer, *Chemical reviews*, 103(12), 4953–4962,
11 2003.

12 Carpenter, L. J., Malin, G. and Liss, P. S.: Novel biogenic iodine-containing trihalomethanes and
13 other, *Global Biogeochemical Cycles*, 14(4), 1191–1204, 2000.

14 Carpenter, L. J., MacDonald, S. M., Shaw, M. D., Kumar, R., Saunders, R. W., Parthipan, R., Wilson,
15 J. and Plane, J. M. C.: Atmospheric iodine levels influenced by sea surface emissions of
16 inorganic iodine, *Nature Geoscience*, 6(2), 108, 2013.

17 Carpenter, L. J., Reimann, S., Burkholder, J. B., Clerbaux, C., Hall, B. D., Hossaini, R., Laube, J. C.,
18 Yvon-Lewis, S. A., Engel, A. and Montzka, S. A.: Update on ozone-depleting substances
19 (ODSs) and other gases of interest to the Montreal protocol, *Scientific assessment of ozone*
20 *depletion: 2014*, 1, 2014.

21 Davis, D., Crawford, J., Liu, S., McKeen, S., Bandy, A., Thornton, D., Rowland, F. and Blake, D.:
22 Potential impact of iodine on tropospheric levels of ozone and other critical oxidants,

1 Journal of Geophysical Research: Atmospheres, 101(D1), 2135–2147, 1996.

2 Duce, R. A., Liss, P. S., Merrill, J. T., Atlas, E. L., Buat-Menard, P., Hicks, B. B., Miller, J. M., Prospero,
3 J. M., Arimoto, R., Church, T. M., Ellis, W., Galloway, J. N., Hansen, L., Jickells, T. D., Knap, A.
4 H., Reinhardt, K. H., Schneider, B., Soudine, A., Tokos, J. J., Tsunogai, S., Wollast, R. and
5 Zhou, M.: The atmospheric input of trace species to the world ocean, *Global*
6 *Biogeochemical Cycles*, 5(3), 193–259, doi:10.1029/91GB01778, 1991.

7 Elliott, S. and Rowland, F. S.: Nucleophilic substitution rates and solubilities for methyl halides in
8 seawater, *Geophysical Research Letters*, 20(11), 1043–1046, 1993.

9 Fuse, H., Inoue, H., Murakami, K., Takimura, O. and Yamaoka, Y.: Production of free and organic
10 iodine by *Roseovarius* spp., *FEMS Microbiology Letters*, 229(2), 189–194,
11 doi:10.1016/S0378-1097(03)00839-5, 2003.

12 Garland, J. A., Elzerman, A. W. and Penkett, S. A.: The mechanism for dry deposition of ozone to
13 seawater surfaces, *Journal of Geophysical Research: Oceans*, 85(C12), 7488–7492, 1980.

14 Giese, B., Laturnus, F., Adams, F. C. and Wiencke, C.: Release of Volatile Iodinated C1– C4
15 Hydrocarbons by Marine Macroalgae from Various Climate Zones, *Environmental science*
16 *& technology*, 33(14), 2432–2439, 1999.

17 Groszko, W. M.: An estimate of the global air-sea flux of methyl chloride, methyl bromide, and
18 methyl iodide, PhD Thesis, Dalhousie University., 1999.

19 Hepach, H., Quack, B., Tegtmeier, S., Engel, A., Bracher, A., Fuhlbrügge, S., Galgani, L., Atlas, E.
20 L., Lampel, J., Frieß, U. and Krüger, K.: Biogenic halocarbons from the Peruvian upwelling
21 region as tropospheric halogen source, *Atmospheric Chemistry and Physics*, 16(18), 12219–
22 12237, doi:10.5194/acp-16-12219-2016, 2016.

- 1 Hill, V. L. and Manley, S. L.: Release of reactive bromine and iodine from diatoms and its possible
2 role in halogen transfer in polar and tropical oceans, *Limnology and Oceanography*, 54(3),
3 812–822, doi:10.4319/lo.2009.54.3.0812, 2009.
- 4 Hughes, C., Malin, G., Turley, C. M., Keely, B. J. and Nightingale, P. D.: The production of volatile
5 iodocarbons by biogenic marine aggregates, *Limnology and Oceanography*, 53(2), 867–872,
6 2008.
- 7 Hughes, C., Franklin, D. J. and Malin, G.: Iodomethane production by two important marine
8 cyanobacteria: *Prochlorococcus marinus* (CCMP 2389) and *Synechococcus* sp.(CCMP 2370),
9 *Marine Chemistry*, 125(1–4), 19–25, 2011.
- 10 Jones, C. E. and Carpenter, L. J.: Solar photolysis of CH_2I_2 , CH_2ICl , and CH_2IBr in water, saltwater,
11 and seawater, *Environmental science & technology*, 39(16), 6130–6137, 2005.
- 12 Jones, C. E. and Carpenter, L. J.: Chemical destruction of CH_3I , $\text{C}_2\text{H}_5\text{I}$, $1\text{-C}_3\text{H}_7\text{I}$, and $2\text{-C}_3\text{H}_7\text{I}$ in
13 saltwater, *Geophysical Research Letters*, 34(13), 1–6, doi:10.1029/2007GL029775, 2007.
- 14 Jones, C. E., Hornsby, K. E., Dunk, R. M., Leigh, R. J. and Carpenter, L. J.: Coastal measurements
15 of short-lived reactive iodocarbons and bromocarbons at Roscoff, Brittany during the
16 RHaMBLe campaign, *Atmospheric Chemistry and Physics*, 9(22), 8757–8769,
17 doi:10.5194/acp-9-8757-2009, 2009.
- 18 Jones, C. E., Hornsby, K. E., Sommariva, R., Dunk, R. M., Von Glasow, R., McFiggans, G. and
19 Carpenter, L. J.: Quantifying the contribution of marine organic gases to atmospheric iodine,
20 *Geophysical Research Letters*, 37(18), L18804, 2010.
- 21 Kerrigan, E. A., Kienast, M., Thomas, H. and Wallace, D. W. R.: Using oxygen isotopes to establish
22 freshwater sources in Bedford Basin, Nova Scotia, a Northwestern Atlantic fjord, *Estuarine*,

- 1 Coastal and Shelf Science, 199, 96–104, 2017.
- 2 Klick, S.: Seasonal variations of biogenic and anthropogenic halocarbons in seawater from a
3 coastal site, *Limnology and oceanography*, 37(7), 1579–1585, 1992.
- 4 Kurihara, M. K., Kimura, M., Iwamoto, Y., Narita, Y., Ooki, A., Eum, Y. J., Tsuda, A., Suzuki, K., Tani,
5 Y., Yokouchi, Y., Uematsu, M. and Hashimoto, S.: Distributions of short-lived iodocarbons
6 and biogenic trace gases in the open ocean and atmosphere in the western North Pacific,
7 *Marine Chemistry*, 118(3–4), 156–170, doi:10.1016/j.marchem.2009.12.001, 2010.
- 8 Li, B.: Changes in Planktonic Microbiota, in *Preserving the environment of Halifax Harbour*, edited
9 by L. William K. W., G. Turner, and A. Ducharme, pp. 105–121., 2001.
- 10 Li, W. K. W.: Annual average abundance of heterotrophic bacteria and *Synechococcus* in surface
11 ocean waters, *Limnology and oceanography*, 43(7), 1746–1753, 1998.
- 12 Liss, P. S. and Slater, P. G.: Flux of Gases across the Air-Sea Interface, *Nature*, 247(5438), 181–
13 184, doi:10.1038/247181a0, 1974.
- 14 Mahajan, A. S., Plane, J. M. C., Oetjen, H., Mendes, L., Saunders, R. W., Saiz-Lopez, A., Jones, C.
15 E., Carpenter, L. J. and McFiggans, G. B.: Measurement and modelling of tropospheric
16 reactive halogen species over the tropical Atlantic Ocean, *Atmospheric Chemistry and
17 Physics*, 10(10), 4611–4624, 2010.
- 18 Mahajan, A. S., Gómez Martín, J. C., Hay, T. D., Royer, S.-J., Yvon-Lewis, S., Liu, Y., Hu, L., Prados-
19 Roman, C., Ordóñez, C. and Plane, J. M. C.: Latitudinal distribution of reactive iodine in the
20 Eastern Pacific and its link to open ocean sources, *Atmospheric Chemistry and Physics*,
21 12(23), 11609–11617, 2012.
- 22 Manley, S. L. and de la Cuesta, J. L.: Methyl iodide production from marine phytoplankton

1 cultures, *Limnology and Oceanography*, 42(1), 142–147, 1997.

2 Martino, M., Liss, P. S. and Plane, J. M. C.: The Photolysis of Dihalomethanes in Surface Seawater,
3 *Environmental Science & Technology*, 39(18), 7097–7101, doi:10.1021/es048718s, 2005.

4 Martino, M., Liss, P. S. and Plane, J.: Wavelength-dependence of the photolysis of
5 diiodomethane in seawater, *Geophysical research letters*, 33(6), L06606,
6 doi:10.1029/2005GL025424, 2006.

7 Martino, M., Mills, G. P., Woeltjen, J. and Liss, P. S.: A new source of volatile organoiodine
8 compounds in surface seawater, *Geophysical Research Letters*, 36(1), L01609,
9 doi:10.1029/2008GL036334, 2009.

10 McFiggans, G., Plane, J., Allan, B. J., Carpenter, L. J., Coe, H. and O’Dowd, C.: A modeling study of
11 iodine chemistry in the marine boundary layer, *Journal of Geophysical Research:*
12 *Atmospheres*, 105(D11), 14371–14385, 2000.

13 McFiggans, G., Coe, H., Burgess, R., Allan, J., Cubison, M., Alfarra, M. R., Saunders, R., Saiz-Lopez,
14 A., Plane, J. M. C. and Wevill, D.: Direct evidence for coastal iodine particles from *Laminaria*
15 macroalgae–linkage to emissions of molecular iodine, *Atmospheric Chemistry and Physics*,
16 4(3), 701–713, 2004.

17 Moore, R. M. and Tokarczyk, R.: Volatile biogenic halocarbons in the northwest Atlantic, *Global*
18 *Biogeochemical Cycles*, 7(1), 195–210, 1993.

19 Moore, R. M. and Zafiriou, O. C.: Photochemical production of methyl iodide in seawater, *Journal*
20 *of Geophysical Research: Atmospheres*, 99(D8), 16415–16420, 1994.

21 Moore, R. M., Geen, C. E. and Tait, V. K.: Determination of Henry’s law constants for a suite of
22 naturally occurring halogenated methanes in seawater, *Chemosphere*, 30(6), 1183–1191,

1 1995.

2 Mössinger, J. C., Shallcross, D. E. and Cox, R. A.: UV–VIS absorption cross-sections and
3 atmospheric lifetimes of CH_2Br_2 , CH_2I_2 and CH_2BrI , Journal of the Chemical Society, Faraday
4 Transactions, 94(10), 1391–1396, 1998.

5 Nightingale, P. D., Malin, G., Law, C. S., Watson, A. J., Liss, P. S., Liddicoat, M. I., Boutin, J. and
6 Upstill-Goddard, R. C.: In situ evaluation of air-sea gas exchange parameterizations using
7 novel conservative and volatile tracers, Global Biogeochemical Cycles, 14(1), 373–387,
8 2000.

9 O’Dowd, C. D., Jimenez, J. L., Bahreini, R., Flagan, R. C., Seinfeld, J. H., Hameri, K., Pirjola, L.,
10 Kulmala, M., Jennings, S. G. and Hoffmann, T.: Marine aerosol formation from biogenic
11 iodine emissions, Nature, 417(6889), 632–636, <http://dx.doi.org/10.1038/nature00775>,
12 2002.

13 Orlikowska, A. and Schulz-Bull, D. E.: Seasonal variations of volatile organic compounds in the
14 coastal Baltic Sea, Environmental Chemistry, 6(6), 495–507, doi:10.1071/EN09107, 2009.

15 Orlikowska, A., Stolle, C., Pollehne, F., Jürgens, K. and Schulz-Bull, D. E.: Dynamics of halocarbons
16 in coastal surface waters during short term mesocosm experiments, Environmental
17 Chemistry, 12(4), 515–525, doi:10.1071/EN14204, 2015.

18 Rasmussen, R. A., Khalil, M. A. K., Gunawardena, R. and Hoyt, S. D.: Atmospheric methyl iodide
19 (CH_3I), Journal of Geophysical Research: Oceans, 87(C4), 3086–3090, 1982.

20 Rattigan, O. V., Shallcross, D. E. and Cox, R. A.: UV absorption cross-sections and atmospheric
21 photolysis rates of CF_3I , CH_3I , $\text{C}_2\text{H}_5\text{I}$ and CH_2ICl , Journal of the Chemical Society, Faraday
22 Transactions, 93(16), 2839–2846, 1997.

1 Richter, U. and Wallace, D. W. R.: Production of methyl iodide in the tropical Atlantic Ocean,
2 Geophysical Research Letters, 31(23), L23S03, doi:10.1029/2004GL020779, 2004.

3 Saiz-Lopez, A. and Von Glasow, R.: Reactive halogen chemistry in the troposphere, Chemical
4 Society Reviews, 41(19), 6448, doi:10.1039/c2cs35208g, 2012.

5 Schall, C., Laturus, F. and Heumann, K. G.: Biogenic volatile organoiodine and organobromine
6 compounds released from polar macroalgae, Chemosphere, 28(7), 1315–1324,
7 doi:10.1016/0045-6535(94)90076-0, 1994.

8 Shan, S., Sheng, J., Thompson, K. R. and Greenberg, D. A.: Simulating the three-dimensional
9 circulation and hydrography of Halifax Harbour using a multi-nested coastal ocean
10 circulation model, Ocean Dynamics, 61(7), 951–976, 2011.

11 Shi, Q., Petrick, G., Quack, B., Marandino, C. and Wallace, D. W. R.: A time series of incubation
12 experiments to examine the production and loss of CH₃I in surface seawater, Journal of
13 Geophysical Research Oceans, (2), 1022–1037, doi:10.1002/2013JC009415, 2014a.

14 Shi, Q., Petrick, G., Quack, B., Marandino, C. and Wallace, D.: Seasonal variability of methyl iodide
15 in the Kiel Fjord, Journal of Geophysical Research: Oceans, 119(3), 1609–1620,
16 doi:10.1002/2013JC009328, 2014b.

17 Shimizu, Y., Ooki, A., Onishi, H., Takatsu, T., Tanaka, S., Inagaki, Y., Suzuki, K., Kobayashi, N.,
18 Kamei, Y. and Kuma, K.: Seasonal variation of volatile organic iodine compounds in the
19 water column of Funka Bay, Hokkaido, Japan, Journal of Atmospheric Chemistry, 74(2),
20 205–225, 2017.

21 Smythe-Wright, D., Boswell, S. M., Breithaupt, P., Davidson, R. D., Dimmer, C. H. and Eiras Diaz,
22 L. B.: Methyl iodide production in the ocean: Implications for climate change, Global

1 Biogeochemical Cycles, 20(3), GB3003, 2006.

2 Solomon, S., Garcia, R. R. and Ravishankara, A. R.: On the role of iodine in ozone depletion,
3 Journal of Geophysical Research: Atmospheres, 99(D10), 20491–20499, 1994.

4 Stemmler, I., Rothe, M., Hense, I. and Hepach, H.: Numerical modelling of methyl iodide in the
5 eastern tropical Atlantic, *Biogeosciences*, 10(6), 4211–4225, 2013.

6 Stemmler, I., Hense, I., Quack, B. and Maier-Reimer, E.: Methyl iodide production in the open
7 ocean, *Biogeosciences*, 11(16), 4459–4476, 2014.

8 Tegtmeier, S., Krüger, K., Quack, B., Atlas, E., Blake, D. R., Bönisch, H., Engel, A., Hepach, H.,
9 Hossaini, R. and Navarro, M. A.: The contribution of oceanic methyl iodide to stratospheric
10 iodine, *Atmospheric Chemistry and Physics*, 13(23), 11869–11886, 2013.

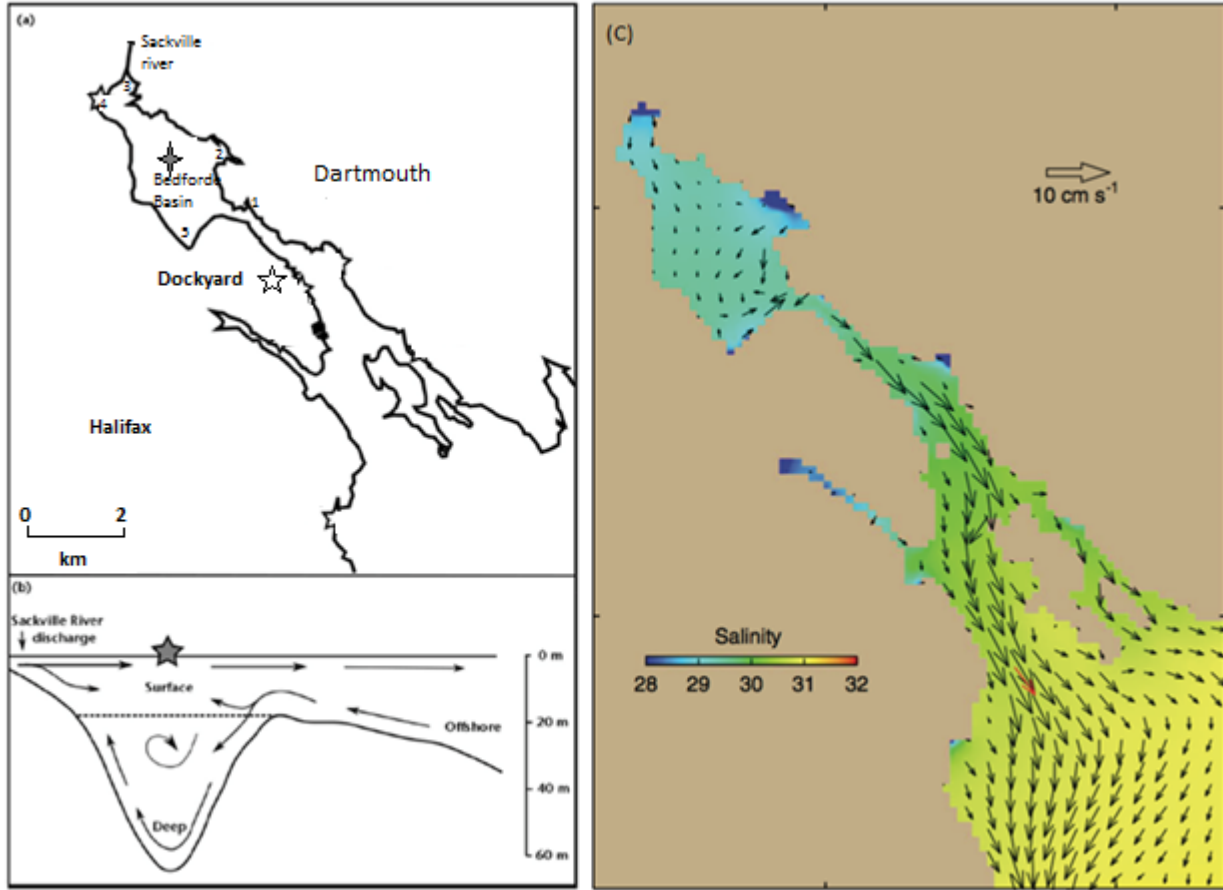
11 Yamamoto, H., Yokouchi, Y., Otsuki, A. and Itoh, H.: Depth profiles of volatile halogenated
12 hydrocarbons in seawater in the Bay of Bengal, *Chemosphere*, 45(3), 371–377,
13 doi:[http://dx.doi.org/10.1016/S0045-6535\(00\)00541-5](http://dx.doi.org/10.1016/S0045-6535(00)00541-5), 2001.

14 Yokouchi, Y., Osada, K., Wada, M., Hasebe, F., Agama, M., Murakami, R., Mukai, H., Nojiri, Y.,
15 Inuzuka, Y. and Toom-Sauntry, D.: Global distribution and seasonal concentration change
16 of methyl iodide in the atmosphere, *Journal of Geophysical Research: Atmospheres*,
17 113(D18), D18311, doi:[10.1029/2008JD009861](https://doi.org/10.1029/2008JD009861), 2008.

18 Yokouchi, Y., Saito, T., Ooki, A. and Mukai, H.: Diurnal and seasonal variations of iodocarbons
19 (CH₂ClI, CH₂I₂, CH₃I, and C₂H₅I) in the marine atmosphere, *Journal of Geophysical Research:*
20 *Atmospheres*, 116(D6), D06301, doi:[10.1029/2010JD015252](https://doi.org/10.1029/2010JD015252), 2011.

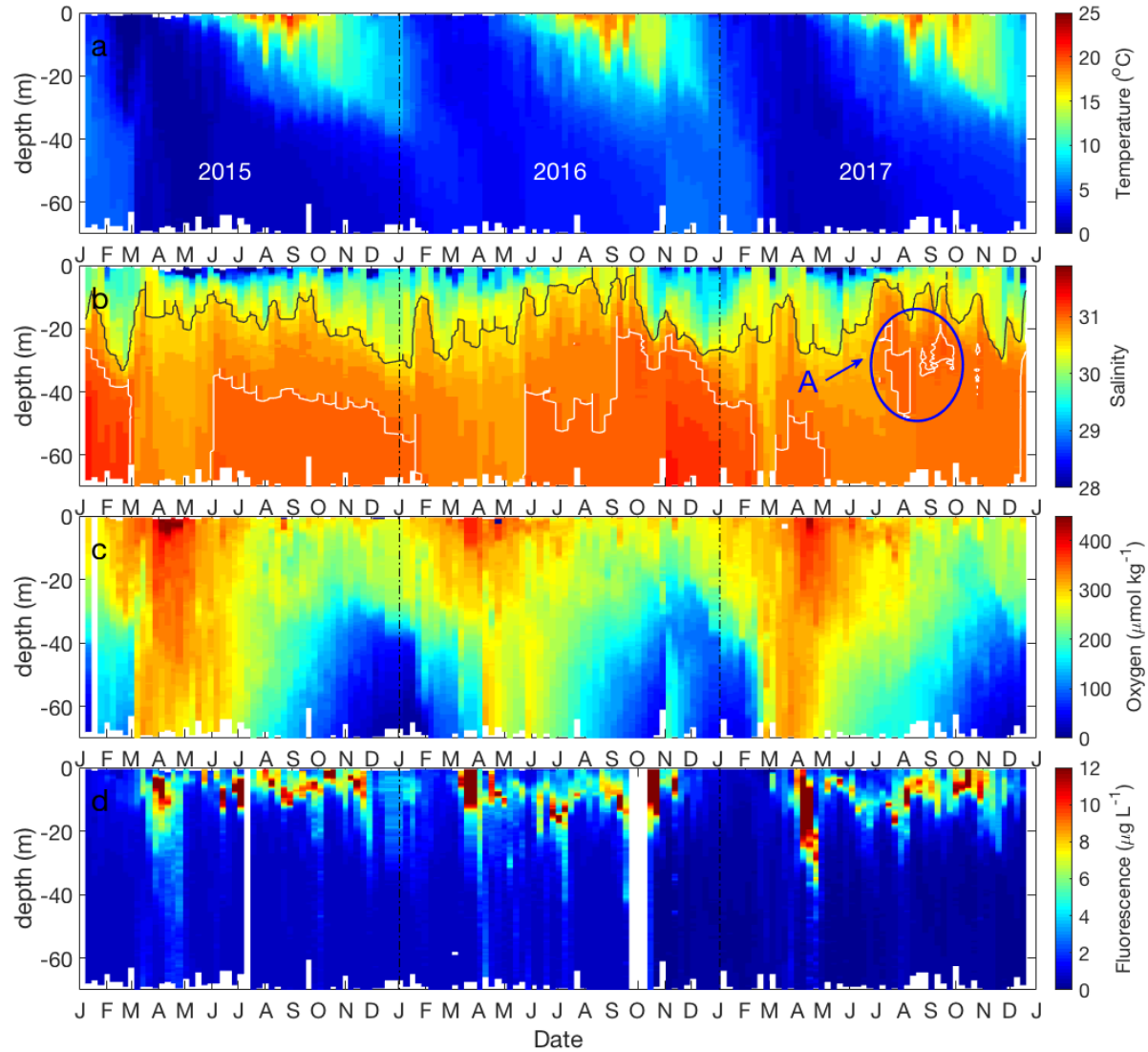
21 Ziska, F., Quack, B., Abrahamsson, K., Archer, S. D., Atlas, E., Bell, T., Butler, J. H., Carpenter, L. J.,
22 Jones, C. E. and Harris, N. R. P.: Global sea-to-air flux climatology for bromoform,

1 dibromomethane and methyl iodide, Atmospheric Chemistry and Physics, 13(17), 8915–
2 8934 <https://doi.org/10.5194/acp-13-8915-2013>, 2013.
3
4
5
6
7
8
9
10
11



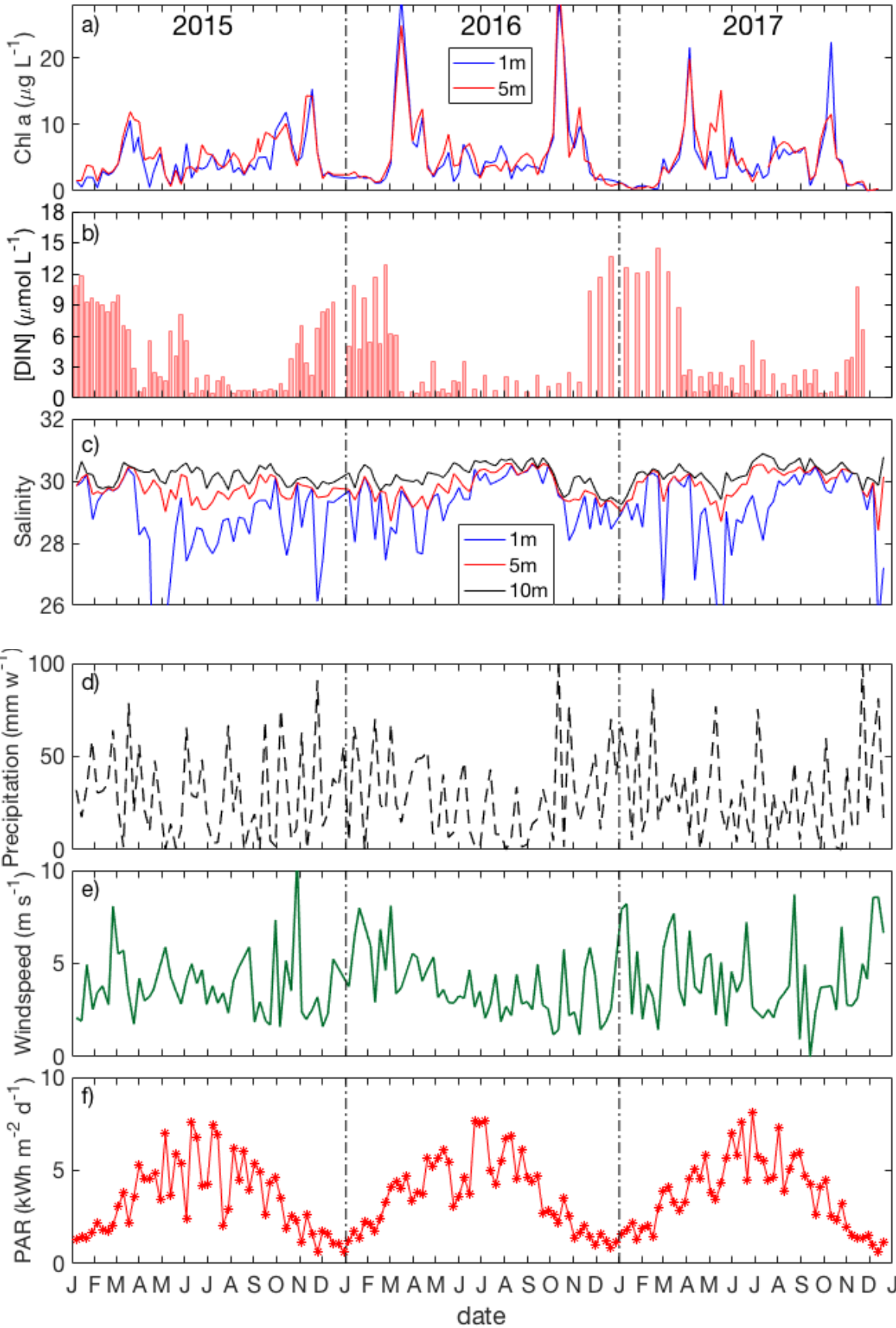
1
2
3
4
5
6

Figure 1. (a): Main sampling location (grey star) and near-shore sampling locations 1-5 (1: Tufts cove; 2: Wrights cove; 3: Sackville; 4: Mill cove; 5: Fairview cove) in Bedford Basin; (b): two layered flow in Halifax Harbour, adapted from Kerrigan et al. (2017); (c): horizontal circulation of water in Halifax Harbour from Shan et al. (2011), using annual mean currents and velocities.



1
2
3
4
5
6
7

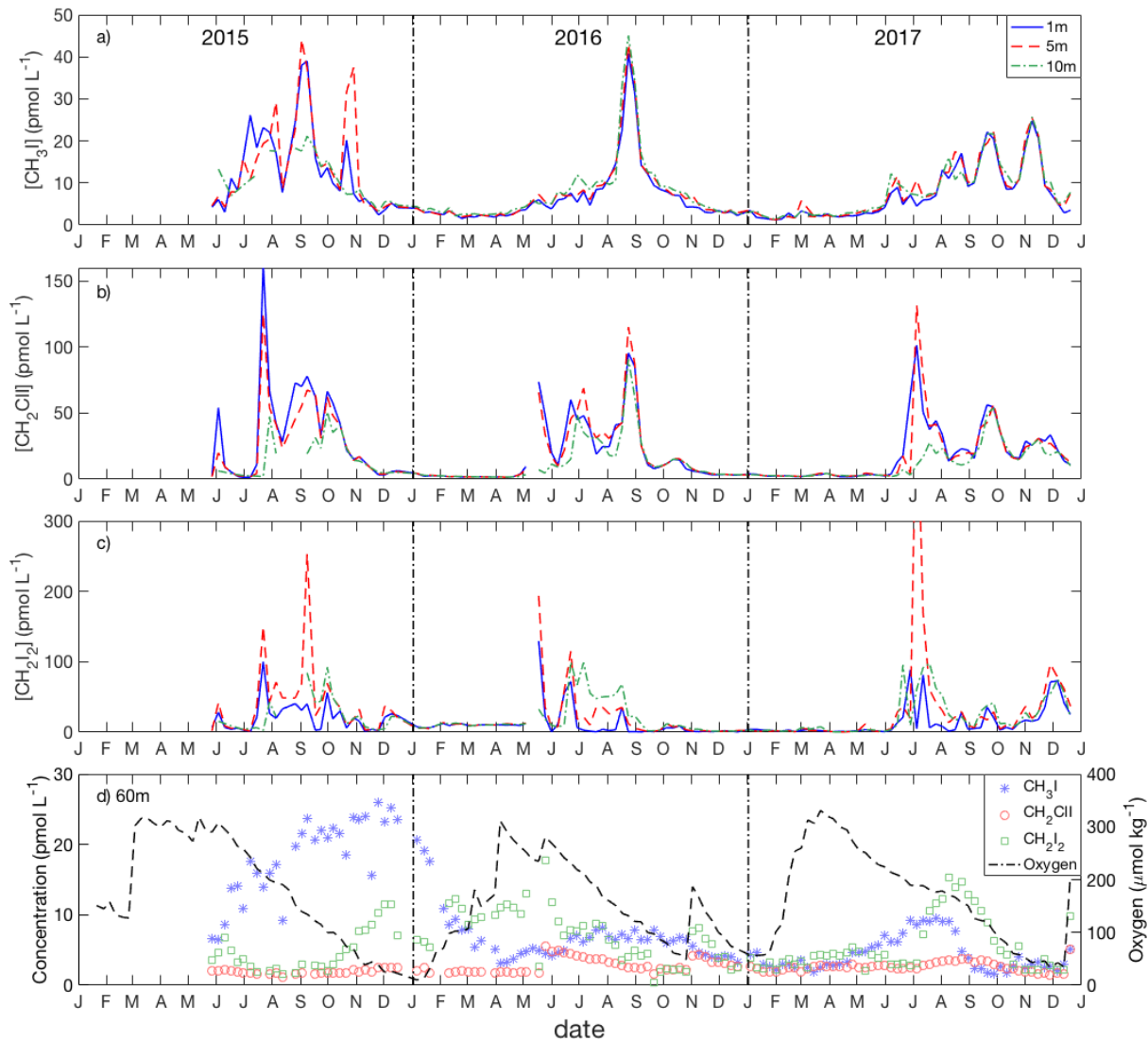
Figure 2. Seasonal patterns of environmental and biological variables in Bedford Basin from January 2015 to Dec 2017. (a) temperature; (b) salinity (grey contour line for S=30.5; white contour line for S=31). The blue circle (A) highlights a mid-depth intrusion. (c) dissolved oxygen; (d) chlorophyll fluorescence.



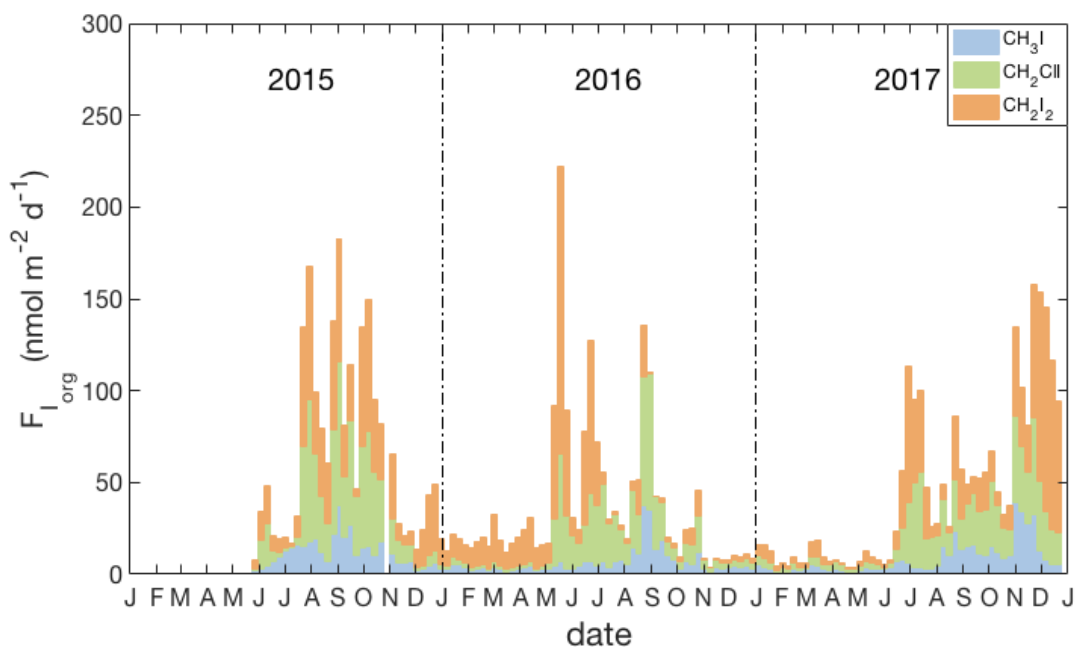
1

2

1 **Figure 3.** Seasonal variation of (a) chlorophyll *a*: 1 m (blue line) and 5 m (red line); (b) DIN; (c)
 2 salinity in the surface layer: 1m (blue line), 5m (red line) and 10m (black line); (d) weekly
 3 precipitation and (e) daily averaged windspeed (shown here only for sampling days); (f) weekly
 4 average PAR from January 2015 to December 2017.
 5
 6
 7
 8

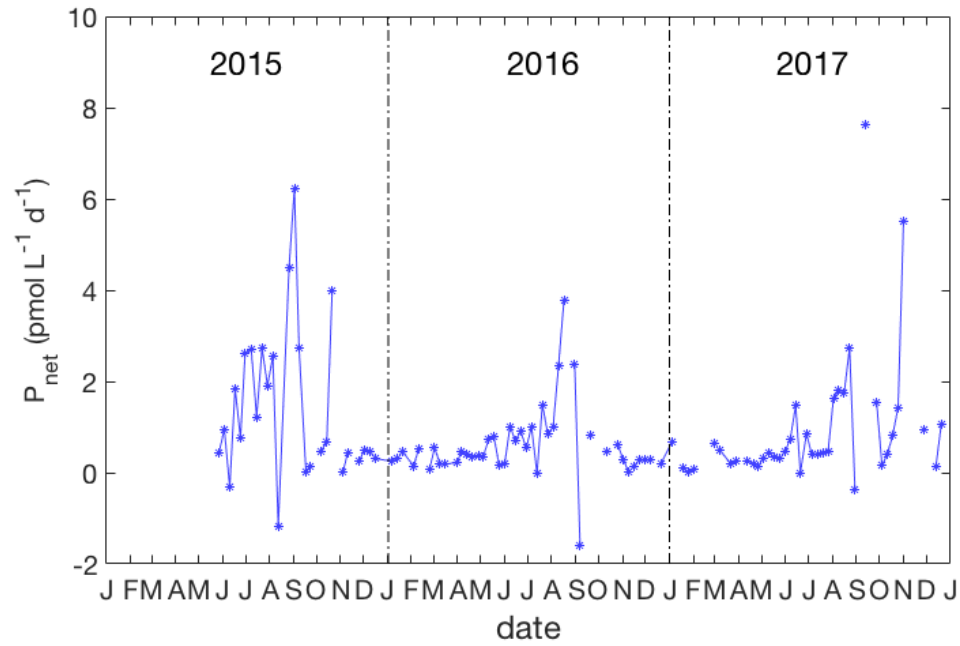


9
 10
 11 **Figure 4.** Seasonal variation of iodocarbons in the Bedford Basin at 1 m (blue line), 5 m (red line)
 12 and 10 m (green line) from May 2015 to December 2017: (a) CH_3I ; (b) CH_2ClI and (c) CH_2I_2 . (d):
 13 time-series from near-bottom water (60m) of iodocarbons and dissolved oxygen.



1
2
3
4
5
6
7
8
9

Figure 5 Weekly averages of daily sea-to-air flux estimates of I_{org} (see section 3.3): including relative contributions of individual compounds (blue: CH_3I , green: CH_2ClI and orange: CH_2I_2) and using the parameterization for transfer velocity (k_w) of Nightingale et al. (2000) and for the airside transfer velocity (k_a) of Duce et al. [1991].

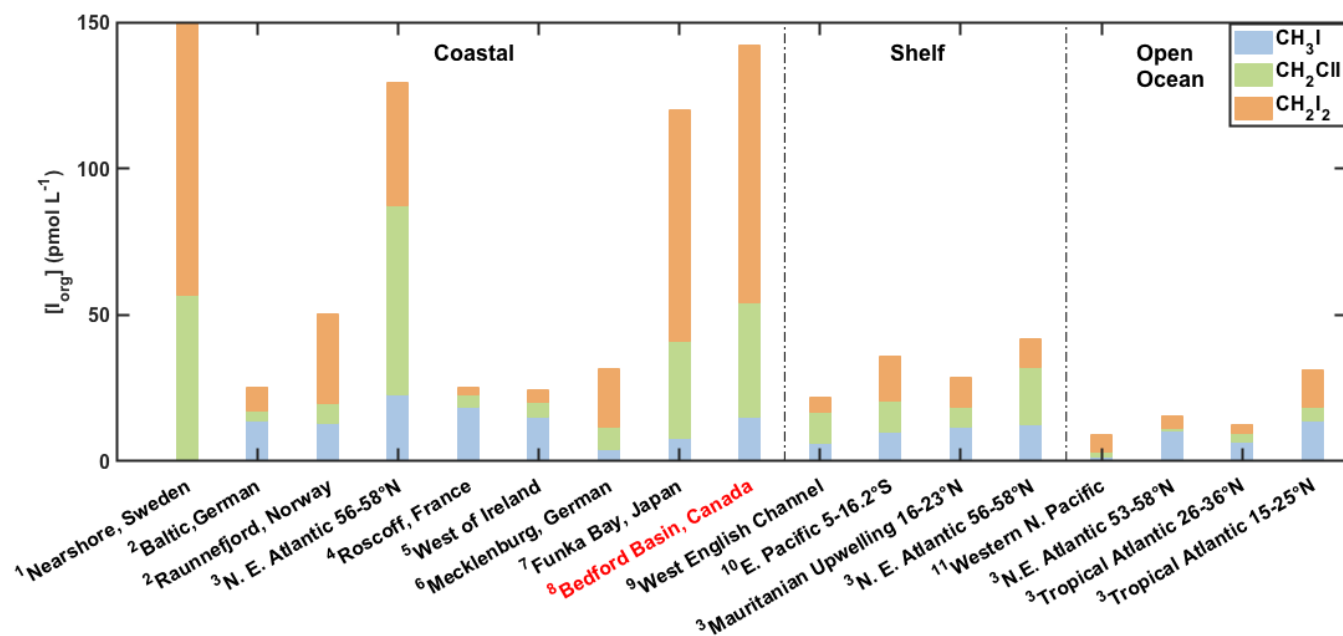


1
2

3 **Figure 6.** Variation of the net production rate of CH₃I in the upper 10 m from 2015 to 2017. No
4 data are plotted when the layer of uniform density extended below 10 m.

5
6
7
8
9
10

1



2

3

4 **Figure 7.** Contribution of Iodocarbons to total organic iodine (I_{org}) in surface seawater from
5 different regions and studies:

6 1: Klick, 1992; 2: Orlikowski et al., 2015; 3: Jones et al., 2010; 4: Jones et al. 2009; 5: Carpenter
7 et al., 2000; 6: Orlikowski & Schulz-Bull, 2009; 7: Shimizu et al., 2017; 8: this study; 9: Archer et
8 al., 2007; 10: Hepach et al., 2016; 11: Kurihara et al., 2010.

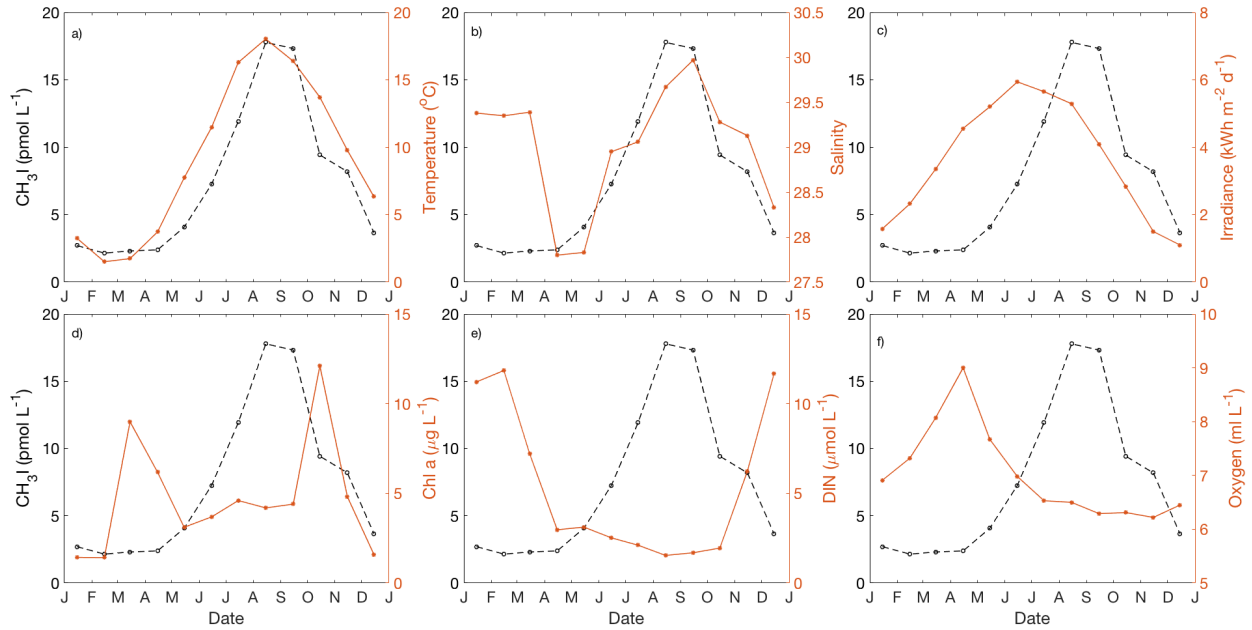
9

10

11

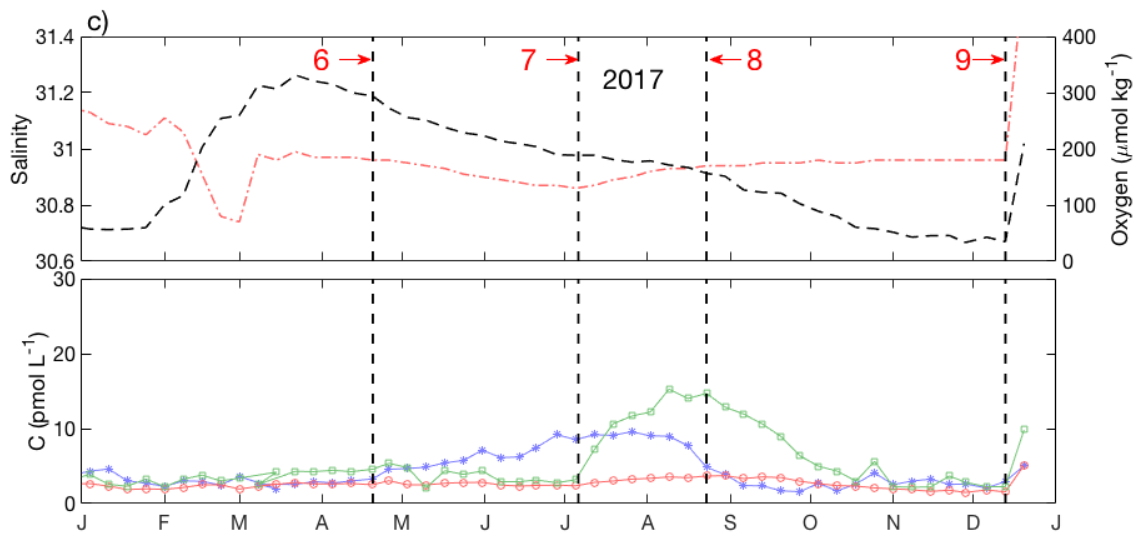
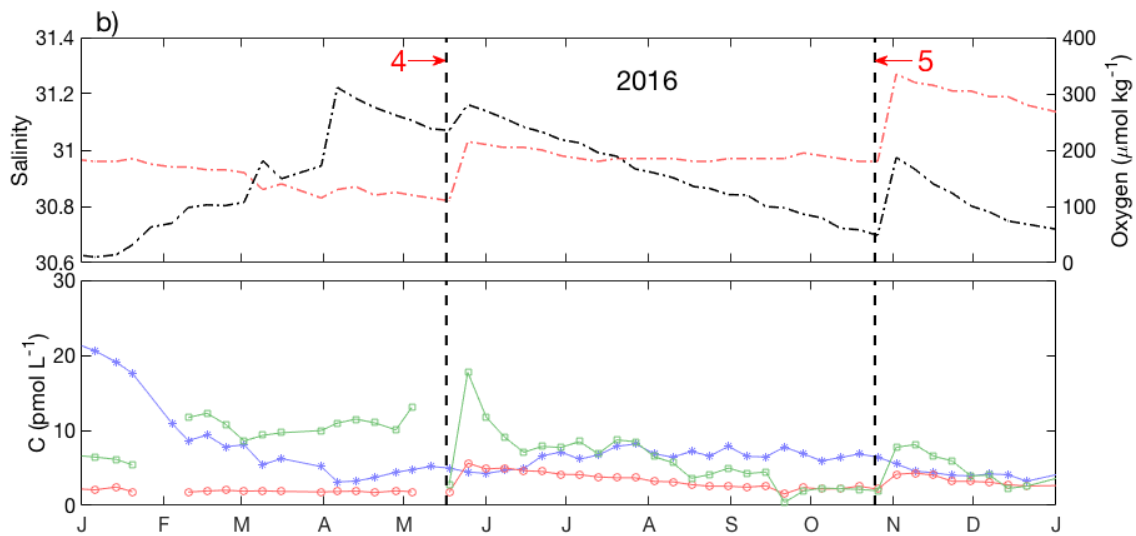
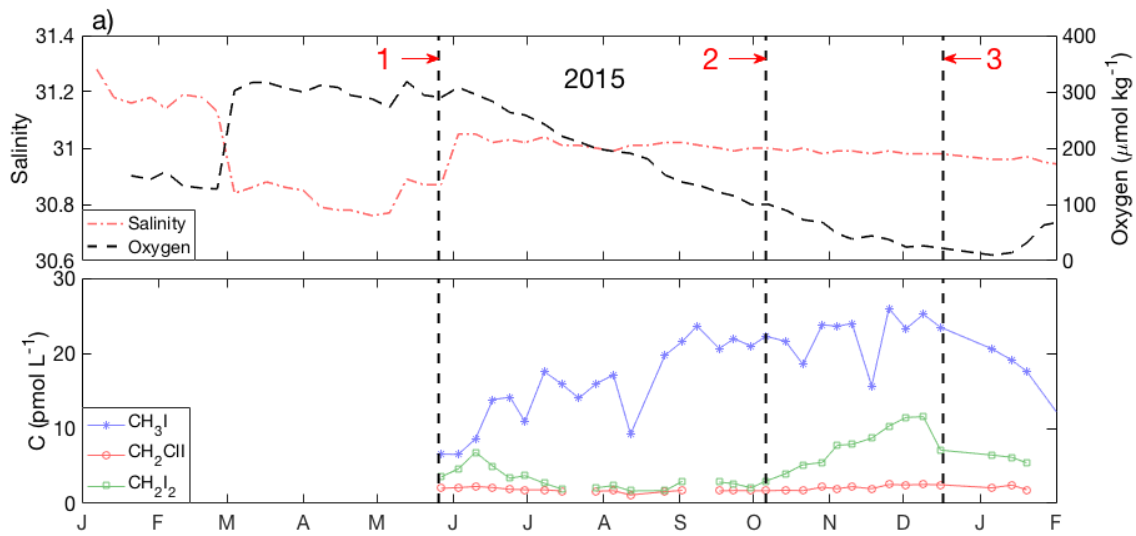
12

13



1
2
3
4 **Figure 8.** Annual cycle of (a) temperature, (b) salinity, (c) irradiance, (d) Chl *a*, (e) dissolved
5 inorganic nitrogen (DIN) and (f) dissolved oxygen for near-surface water (1-5 m) in Bedford Basin.
6 The black dashed line depicts the annual cycle of CH₃I. The figures present the monthly mean
7 values based on the data collected from May 2015 to December 2017.

8
9
10
11
12
13
14
15
16
17
18
19
20
21



1 **Figure 9.** Detailed time-series from near-bottom waters in (a) 2015, (b) 2016 and (c) 2017. For
 2 each year, the upper panel shows variability of salinity (red dash-dot line) and dissolved oxygen
 3 (black dashed line); the lower panel shows iodocarbons (CH_3I : blue stars; CH_2ClI : red open circles
 4 and CH_2I_2 : green open squares). The vertical bold, dashed lines (1 to 9) represent special events
 5 discussed in section 4.5.

6
7

8

9

10

11 **Table 1.** R^2 value (Pearson's correlation coefficients, $p < 0.05$) for the individual iodocarbon data
 12 based on both weekly data and monthly average.

	weekly			monthly		
	CH_3I	CH_2ClI	CH_2I_2	CH_3I	CH_2ClI	CH_2I_2
CH_3I (1m)	1.0			1.0		
CH_2ClI (1m)	0.4	1.0		0.7	1.0	
CH_2I_2 (1m)	0.0	0.3	1.0	0.1	0.4	1.0
CH_3I (5m)	1.0			1.0		
CH_2ClI (5m)	0.4	1.0		0.5	1.0	
CH_2I_2 (5m)	0.1	0.4	1.0	0.1	0.6	1.0
CH_3I (10m)	1.0			1.0		
CH_2ClI (10m)	0.7	1.0		0.7	1.0	
CH_2I_2 (10m)	0.1	0.3	1.0	0.2	0.4	1.0

13

14

15

16

17

1 **Table 2.** R² value (pearson's correlation coefficients, p<0.05) for iodocarbons and potentially
 2 relevant parameters based on both weekly data and monthly average.

	weekly			monthly		
1m	<i>CH₃I</i>	<i>CH₂ClI</i>	<i>CH₂I₂</i>	<i>CH₃I</i>	<i>CH₂ClI</i>	<i>CH₂I₂</i>
SST	0.5	0.4	0.0	0.7	0.6	0.1
SSS	0.1	0.0	0.0	0.1	0.1	0.0
Oxygen	0.3	0.2	0.1	0.3	0.2	0.1
Flu	0.0	0.0	0.0	0.1	0.0	0.0
PAR	0.1	0.1	0.0	0.1	0.3	0.0

3
 4
 5
 6
 7
 8
 9
 10
 11
 12
 13
 14
 15
 16
 17

1 **Table 3.** Seasonal variation of total sea-to-air fluxes of iodocarbons ($\text{nmol m}^{-2} \text{d}^{-1}$). Highest flux
 2 values of iodocarbons in each year are marked in red.

year	season	CH ₃ I	CH ₂ ClI	CH ₂ I ₂	I _{org}
2015	Spring				
	Summer	13.9	29.3	15.4	74.0
	Fall	13.1	30.7	13.7	71.2
	Winter	3.6	3.0	8.6	23.7
	Annual	11.9	25.9	14.0	65.9
2016	Spring	3.4	11.8	16.5	48.2
	Summer	12.0	33.2	9.4	64.0
	Fall	7.2	9.4	1.8	20.2
	Winter	3.2	3.0	1.7	9.6
	Annual	6.6	14.4	8.2	37.3
2017	Spring	3.0	2.7	1.7	9.0
	Summer	7.8	22.1	12.1	54.1
	Fall	19.7	31.3	15.9	82.8
	winter	3.2	4.5	9.1	25.9
	Annual	8.5	15.9	10.1	44.7

3
 4
 5
 6
 7
 8
 9
 10
 11
 12
 13

1 **Table 4.** Concentration (pmol L⁻¹) of iodocarbons measured at near shore locations around
2 Bedford Basin as well as at the regular sampling location on July 19, 2017 (1: Tufts cove, 2:
3 Wrights cove, 3: Sackville (rive), 4: Mill cove and 5: Fairview cove) (see Fig. 1a). “Centre” refers
4 to the regular sampling site for the weekly time-series.

5 *Centre Mean for July: the average (and std. deviation) of measurements at the regular, weekly
6 sampling location during the month of July 2017 (n=4).

7

	CH ₃ I	CH ₂ ClI	CH ₂ I ₂
¹ Tufts cove	5.8	35.5	8.8
² Wright's cove	6.7	20.6	12.5
³ Sackville	3.8	6.5	4.9
⁴ Mill cove	8.3	28.0	18.6
⁵ Fairview cove	6.2	26.3	6.4
Middle of Bedford Basin	6.1	37.6	6.3
*Centre Mean for July	5.9±0.9	58.5±25.2	26.1±32.0

8

9

10

11

12

13

14

15

16

17

18

19

1 **Table 5.** Comparison of sea-to-air flux ($\text{nmol m}^{-2} \text{d}^{-1}$) of total organic iodine from different studies.
 2 English Channel is an average for 1 year; Funka Bay value is average over 3 years; Kiel Fjord is
 3 average over 2 years but for CH_3I only; Bedford Basin (this study) is an average over 3 years.
 4 Seasons as defined in this study (see section 2). For Funka Bay, values in parentheses represent
 5 fluxes that have been adjusted from the original reported values to take into account effect of
 6 air-side resistance, using correction factors of 12 and 28 % for CH_2ClI and CH_2I_2 respectively
 7 (based on average effects reported in Archer et al. (2007) and this study; see section 4.6).

8

	English Channel		Funka Bay		Kiel Fjord		Bedford Basin	
	Archer et al.(2007)		Shimizu et al. (2017)		Shi et al. (2014)		This Study	
Season	Total	%- CH_3I	Total	%- CH_3I	Total	%- CH_3I	Total	%- CH_3I
Spring			15.3(12.8)	33.8(40.3)	2.8		28.6	11.1
Summer			113.3(86.6)	4.7(6.2)	5.2		64.0	17.5
Fall			47.6(41.1)	32.5(37.6)	2.2		58.1	23.0
Winter			27.5(22.5)	22.3(27.2)	0.2		19.7	16.8
Annual	42.6	27.9	54.8(43.5)	14.0(17.6)	3.3		46.7	19.3

9

10

11